Mass/Heat-Exchange Network Representation of Distillation Networks

Miguel J. Bagajewicz and Vasilios Manousiouthakis
Dept. of Chemical Engineering, University of California, Los Angeles, CA 90024

This article introduces the "state space" conceptual framework to process synthesis, which is used to provide a novel representation of a distillation network as a composite heat- and mass-exchange network. This representation suggests that distillation network synthesis may best be viewed as an interacting heat- and mass-exchange network synthesis problem. In that regard, familiar tools (such as pinch diagrams) from both heat-exchange network (HEN) and mass-exchange network (MEN) synthesis are shown to be of use in arriving at energy-efficient distillation network designs. Examples of propylene-propane and solvent-water separations are used to illustrate the proposed conceptual framework.

Introduction

Distillation is one of the most important and commonly used separation processes and accounts for a substantial portion of worldwide energy consumption. Distillation networks abound in a number of plants (chemical, petrochemical, microelectronic manufacturing, food, waste recycling, and others), and are used both for valuable product purification/separation and for waste recycling.

Distillation, as well as crystallization and evaporation, is an example of energy-separating-agent processes, which contrast with mass-separating-agent processes (King, 1980) such as absorption, desorption, and ion-exchange. These two classes of separations have traditionally been studied separately.

Methods to design a single distillation column with one feed and two products have been known for years. The McCabe-Thiele and Ponchon-Savarit methods for binary distillation and the Fenske, Underwood, Thiele-Geddes and Lewis-Matheson methods for multicomponent distillation are prominent examples. Design methods for distillation networks with multiple columns, multiple feed and/or product streams, as well as multiple target compositions for multicomponent mixtures, are the subject of intense research efforts.

The task of synthesizing a separation system, of which distillation is a special case, can be defined in a general way as follows: *Given a set of multicomponent streams of known properties, a set of heating, cooling and power supplying utilities and a set of mass-separating agents which may need to be regenerated, it is desired to identify a network of heat/mass exchangers that can yield, with the help of auxiliary equipment such as phase separators, pumps and compressors, a set of multicomponent product streams of desired properties at a minimum venture cost.*

Distillation is not mentioned as such in this definition, being replaced by the more general term "*network of heat/mass exchangers.*" By doing so, the scope of previous definitions of the problem (Rudd and Watson, 1968; Nath and Motard, 1978; Nishida et al., 1981; Westerberg, 1985) is enlarged, including the possibility of using classical distillation one-feed, two-product columns, but also allowing the usage of mass-separating agents, the incorporation of power-supplying utilities such as compressors, the undertaking of the separation task at various pressure levels and the usage of thermodynamic cycles such as heat pumps.

Driven by the energy crisis of the 70s, minimization of utility consumption has been the primary goal of process design for many years. In particular, in heat exchanger network (HEN) synthesis, different methods to determine minimum utility consumption were presented. They have been summarized in two important review papers (Nishida et al., 1981; Gundersen and Naess, 1988).

Westerberg (1985) reviewed the problem of distillation-based separation systems revealing that the literature primarily addressed the separation of a "*single relatively ideal mixture into sharply split, usually pure-component products using systems of single-feed, two-product distillation columns.*" Heat integration of distillation columns has also been discussed in the context of separation system design as far back as 1974 (Rat-

Correspondence concerning this article should be addressed to V. Manousiouthakis.

hore et al., 1974a,b). Many articles have analyzed the problem of using such tools as branch and bound (Morari and Faith, 1980), evolutionary design (Nath and Motard, 1981; Umeda et al., 1979a,b), thermodynamic availability (Naka et al., 1982), pinch design (Dundorf and Linnhoff, 1982; Linnhoff et al., 1983) and utility bounding (Andrecovich, 1983; Andrecovich and Westerberg, 1985), among others.

The concept of superstructure was introduced for distillation trains by Sargent and Gaminibandara (1976) and for heat exchanger networks by Grossmann and Sargent (1978). These superstructures contain many design alternatives and can be used to obtain locally optimal configurations via MINLP programming techniques (Papoulias and Grossmann, 1983a,b,c; Grossmann, 1985; Duran and Grossmann, 1986; Floudas, 1987). Some unsuccessful attempts were made to identify global optima of these types of process synthesis problems. In particular, the application of Generalized Benders Decomposition, as proposed by Floudas et al. (1989) cannot guarantee global optimality and may render local optima or points that are not even extrema (Bagajewicz and Manousiouthakis, 1991; Sahinidis and Grossmann, 1991).

Side strippers and enrichers (Carlberg and Westerberg, 1989a), the Petlyuk configuration (Petlyuk et al., 1965; Carlberg and Westerberg, 1989b), intermediate cooling and heating (Terranova and Westerberg, 1989), multifeed and multiproduct streams (Floudas and Paules IV, 1988; Floudas and Anastasiadis, 1988), azeotropic distillation (Knight and Doherty, 1989), multiple-feed/side streams (Nikolaides and Malone, 1987), nonsharp separations (Maraki and Hayakawa, 1988; Wehe and Westerberg, 1990; Mallick, 1991) are some of the aspects of the general problem currently under study.

As outlined above, research on this subject has been successful in studying particular aspects of the distillation network synthesis problem. Nevertheless, it has not materialized in a comprehensive conceptual framework that can address the problem in its entirety.

To address the separation network synthesis task for the class of problems that employ mass-separation agents, the notion of mass exchange network (MEN) synthesis has been recently proposed (El-Halwagi and Manousiouthakis, 1989a,b; 1990a,b). The design goal of minimizing mass-separating agent cost is attained without prior commitment to any particular design. Pinch points in the design are also found. Finally, networks featuring a minimum number of units are obtained.

It has been common practice in synthesizing distillation networks to first determine the separation sequence and then analyze the possibilities of heat integration. This strategy often provides good designs, though it has been established that the possibilities of heat integration in a flowsheet can alter the optimal separation system design (Linnhoff et al., 1983).

The use of heat pumps in distillation has also been investigated, and their usage has been proven to provide substantial energy savings. Null (1976) has proposed three methods to design distillation columns employing heat pumps: (i) heat pump involving an external fluid; (ii) heat pump using compression of the overhead vapor; and (iii) heat pump using flashing of the reboiler liquid. Studies on the use of heat pumps for distillation columns in the context of overall process heat integration reveal that heat pumping results in energy savings only if heat is pumped across the pinch (Linnhoff et al., 1983; Smith and Linnhoff, 1983). The use of heat pumps in connection with side-stream return and side-stream heating and cooling was also investigated recently (Lynd and Greitland, 1986; Bjorn et al., 1991).

The primary limitation of all existing approaches to distillation network synthesis stems from the inability of these approaches to capture effectively design alternatives which have proven of value in practice. Some approaches ignore heat integration and some assume sharp splits, while others ignore intercooling/interheating and other possibilities and all use the traditional one-feed, two-product stream arrangement. Such limiting assumptions prevent these methodologies from quantifying the minimum utility cost that must be expended for a given separation task to be accomplished using distillation technology.

Although energy savings was the main target of the majority of the studies mentioned, the important question of an *a-priori* minimum utility calculation for distillation networks was not even posed explicitly in the past. There, however, were some attempts to address the issue. Utility bounds were used to develop energy-integrated solutions for the case of multi-effect distillation (Andrecovich, 1983; Andrecovich and Westerberg, 1983). Stream bypassing was also considered as a means of reducing the energy consumption (Wehe and Westerberg, 1987). To allow for more heat recovery, Umeda et al. (1979a) proposed to observe the pinch that develops in the HEN associated to the process and then change process conditions using a set of heuristics. To obtain energy-efficient designs, Kaibel et al. (1989) proposed an evolutionary approach starting from thermodynamically ideal cases, applying certain simplifications, and taking into account the interaction between the heat and mass exchange. In these designs, however, alternatives to the basic mass-transfer arrangement of one-feed, two-product structures were not explored.

To address these deficiencies we propose a significant conceptual departure from previous approaches to distillation network synthesis. The focus of this article is to develop a methodology that addresses the problem of determining distillation alternatives that are energy-efficient for a separation problem with single-component targets. We start first with an introduction to the *state space approach* to process synthesis. We then employ this framework to provide an interacting heat/mass-exchanger network representation of a distillation network. Finally, we examine the interactions between the HEN and the MEN associated with a distillation network, and show how this novel conceptual framework can be used to design energy-efficient distillation networks.

State Space Approach to Process Synthesis

State space notion

In this section, some of the basic concepts that help establish the conceptual framework termed "system theory" are reviewed. In particular, we focus on those primitives necessary for the introduction of the notion of "State Space." An excellent discussion of this subject is given by Zadeh and Desoer (1979).

The behavior of any system can be described quantitatively in terms of a set of variables (density, concentration, temperature, pressure, and so on) and a set of relations among these variables. If the variable set is partitioned in two subsets (input variable and output variable sets), then the aforementioned

system defining relations among these variables are referred to as input-output (I-O) relations. The sets over which input and output variables can assume their values are in turn referred to as input and output spaces.

Input-output (I-O) relations are such that knowledge of the inputs and the I-O relations does not provide knowledge of the output. Any set of variables whose knowledge, when complemented with knowledge of the system inputs and the I-O relations, uniquely determines the system outputs is therefore referred to as a set of state variables. The set over which state variables assume their values is in turn referred to as state space, and the relations which help establish output uniqueness based on state knowledge are referred to as input-state-output (I-S-O) relations.

To illustrate these concepts we consider a single-input, single-output, linear, time-invariant system. Let u and w be scalar-valued time functions on $[t_0, \infty)$ which denote the system input and output variables, respectively. The system defining equations:

$$\sum_{i=0}^{n-1} \alpha_i w^{(i)}(t) + w^{(n)}(t) = \sum_{j=0}^{n-1} \beta_j u^{(j)}(t) \tag{1}$$

$$u^{(j)}(t_0) = 0 \qquad \forall j \tag{2}$$

are the I-O relations. The input and output spaces are the linear vector spaces of scalar valued piecewise infinitely differentiable functions defined on $[t_0, \infty)$.

The theory of ordinary differential equations suggests that knowledge of the input u and of the input-output relation is not sufficient to uniquely determine the output w. Indeed, unique determination of w on $[t_0, \infty)$ requires knowledge of $w(t_0)$ and its derivatives $w^{(i)}(t_0)$, for $i = 1, \ldots, (n-1)$. Therefore, the state space is R^n and the relations given by Eqs. 1-2 and the following initial conditions:

$$w^{(i)}(t_0) = w_0^i \qquad i = 0, \ldots (n-1) \tag{3}$$

are the input-state-output (ISO) relations.

The ISO relations describing any given system are not unique. For example, the aforementioned system can also be defined through another set of ISO relations that can be derived as follows.

We first define the following variables:

$$\left.\begin{aligned}
z_1 &\triangleq w \\
z_2 &\triangleq \dot{z}_1 + \alpha_{n-1} z_1 - \beta_{n-1} u = w^{(1)} + \alpha_{n-1} w - \beta_{n-1} u \\
z_3 &\triangleq \dot{z}_2 + \alpha_{n-2} z_1 - \beta_{n-2} u = w^{(2)} + \alpha_{n-1} w^{(1)} + \alpha_{n-2} w \\
&\qquad - \beta_{n-1} \dot{u} - \beta_{n-2} u \\
&\vdots \\
z_n &\triangleq \dot{z}_{n-1} + \alpha_1 z_1 - \beta_1 u = w^{(n-1)} + \sum_{i=1}^{n-1} \alpha_i w^{(i-1)} \\
&\qquad - \sum_{j=1}^{n-1} \beta_j u^{(j-1)}
\end{aligned}\right\} \tag{4}$$

and then require that:

$$\dot{z}_n \triangleq -\alpha_0 z_1 + \beta_0 u = -\alpha_0 w + \beta_0 u \tag{5}$$

These relations ensure that:

$$\dot{z}_n \triangleq -\alpha_0 w + \beta_0 u = \sum_{i=1}^{n-1} \alpha_i w^{(i)}(t) + w^{(n)}(t) - \sum_{j=1}^{n-1} \beta_j u^{(j)}(t) \tag{6}$$

which is the IO relation of the considered system.

The above equations can be summarized as:

$$\dot{z} \triangleq \begin{bmatrix} \dot{z}_1 \\ \dot{z}_2 \\ \vdots \\ \dot{z}_{n-2} \\ \dot{z}_{n-1} \\ \dot{z}_n \end{bmatrix} = \begin{bmatrix} -\alpha_{n-1} & 1 & 0 & \cdots & 0 & 0 \\ -\alpha_{n-2} & 0 & 1 & \cdots & 0 & 0 \\ \vdots & \vdots & \vdots & \ddots & \vdots & \vdots \\ -\alpha_2 & 0 & 0 & \cdots & 1 & 0 \\ -\alpha_1 & 0 & 0 & \cdots & 0 & 1 \\ -\alpha_0 & 0 & 0 & \cdots & 0 & 0 \end{bmatrix} \begin{bmatrix} z_1 \\ z_2 \\ \vdots \\ z_{n-2} \\ z_{n-1} \\ z_n \end{bmatrix} + \begin{bmatrix} \beta_{n-1} \\ \beta_{n-2} \\ \vdots \\ \beta_2 \\ \beta_1 \\ \beta_0 \end{bmatrix} u \triangleq Az + Bu \tag{7}$$

$$w \triangleq z_1 = [1 \ 0 \ \cdots \ 0 \ 0] \begin{bmatrix} z_1 \\ z_2 \\ \vdots \\ z_{n-1} \\ z_n \end{bmatrix} + [0]u \triangleq Cz + Du \tag{8}$$

$$z(t_0) \triangleq \begin{bmatrix} z_1(t_0) \\ z_2(t_0) \\ \vdots \\ z_{n-1}(t_0) \\ z_n(t_0) \end{bmatrix} = \begin{bmatrix} w \\ \dot{u} + \alpha_{n-1} w - \beta_{n-1} u \\ \vdots \\ w^{(n-2)} + \sum_{i=2}^{n-1} \alpha_i w^{(i-2)} - \sum_{j=2}^{n-1} \beta_j u^{(j-2)} \\ w^{(n-1)} + \sum_{i=1}^{n-1} \alpha_i w^{(i-1)} - \sum_{j=1}^{n-1} \beta_j u^{(j-1)} \end{bmatrix} \tag{9}$$

Since one can uniquely determine w on $[t_0, \infty)$, based on Eqs. 7-9, it is justifiable to characterize these as ISO relations for Eq. 1. The resulting state space is again R^n. The state of the system at t_0 is $z(t_0)$ as defined by Eq. 9. The system state at any time t, $z(t)$, can be evaluated based on the input u, the system state at an earlier time, $z(t_0)$, and some of the ISO relations termed "state equations," $\dot{z} = Az + Bu$. The above state space realization is termed the "observer canonical form" (Kailath, 1980, p. 50) and is often used to establish the notion of observability for linear dynamical systems.

Having provided an algebraic derivation of ISO relations for Eq. 1, we now proceed to a graphical representation of these developments. The derived ISO relations can be represented as shown in Figure 1. This figure can be redrawn by isolating the algebraic operations performed by A, B, C, D

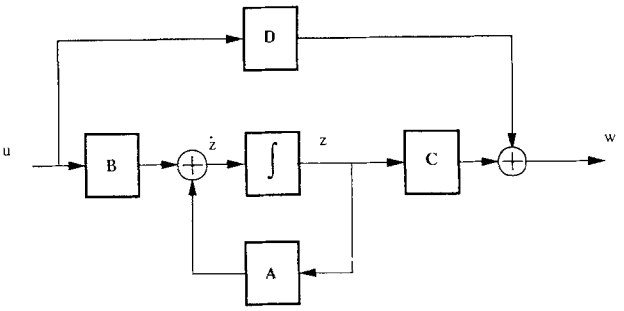

Figure 1. I-S-O representation of a dynamical system.

from the integration operation. The resulting representation is shown in Figure 2. The subsystem represented by:

$$\begin{bmatrix} A & B \\ C & D \end{bmatrix}$$

is a linear finite dimensional operator that processes the input and the state information to generate the output and state derivative information. On the other hand, the input and output of the integration operator $\int$ are the state derivative and state information, respectively.

Implications for process network analysis and synthesis

Having outlined the notion of state space for linear dynamical systems, we are now in a position to examine its implications for the synthesis of chemical process networks. The analysis and synthesis of these systems require that the representation of their input-state-output relations be developed. At the analysis level, the engineer is given the input data u (the raw material) and the I-S-O relations (the network itself), and is asked to predict the output w (the product). At the synthesis level, the engineer is given input data u and output specifications w (that is, IO information), and is asked to develop ISO relations that satisfy these data and specifications. Sometimes, the engineer is given incomplete set of data and specifications; in addition to specifying the ISO relations, he is also asked to provide the missing input data and/or output specifications. One good example of this to determine the optimum utility usage in heat-exchanger network design.

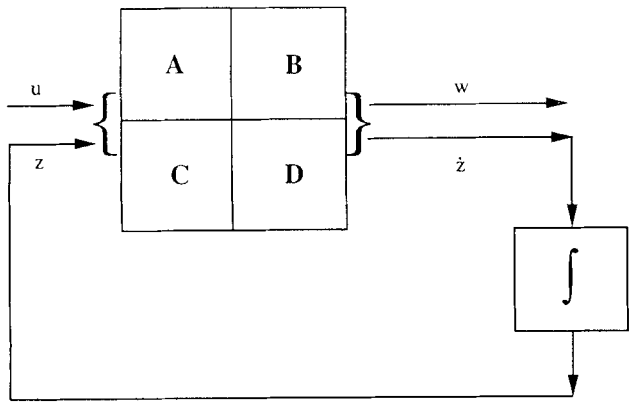

Figure 2. Alternative I-S-O representation of a dynamical system.

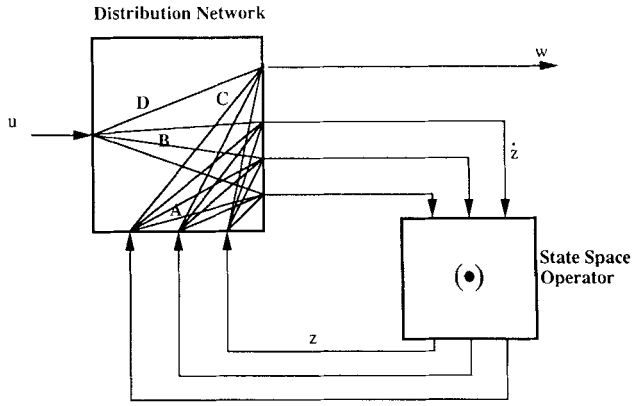

Figure 3. State-space representation.

In this context, one may state that the most challenging goal of process network synthesis is to identify properties shared by *all* ISO relations that can possibly realize given IO information. To pursue this goal one must first provide a systematic way of generating state-space realizations for process networks. For linear dynamical systems, we saw earlier that the interaction of two operators (the integration $\int$ and the ABCD operators) can accomplish this goal. It is our contention that this is also the case for process networks.

Process networks are complex systems whose function is the transformation of certain entities (mass, momentum, and energy) from one state to another. This overall function is attained through decomposition into simpler functions that can be physically realized in a straightforward manner. For example, the function of stream splitting can be realized through a T-type pipe junction, the function of heat transfer can be realized through a countercurrent heat exchanger, and so on. One can classify these functions in two categories:

a. Mixing and splitting
b. Unit operations.

A subsystem that consists of only mixing and splitting functions is a special case of the ABCD operator used in dynamical systems (a special case since the coefficients in the matrices A, B, C and D can be only between 0 and 1, for example) and will be termed a *distribution network* (DN).

The subsystem that either consists of or assesses the impact of unit operations corresponds to the integration operator in linear dynamical systems and gives rise to a process operator (•). The resulting state-space representation of a process network is shown in Figure 3. Streams entering the operator are transformed by it and exit directly opposite to their entrance point.

It is important to realize that:

- The linearity of the I-S-O relations used to establish the analogy is lost.
- The state variables need not be considered functions of time, since process network synthesis problems are mostly concerned with steady-state operations.
- In the I-S-O representation for dynamical systems, the operator is linear (integrator), whereas in the state-space approach to process synthesis, the operator is in general nonlinear.

To better understand how a process network may be rep-

Table 1. Heat-Exchange Network Stream Data (One-Hot, One-Cold and One-Cooling Utility Stream)

Stream	Flow (kg/s)	T_{in} (°C)	T_{out} (°C)
H	1	100	40
C	1	45	65
W	2	15	35

cp = 4.184 kJ/kg·°C; minimum approach temp. = 5°C.

resented in state-space form we consider a heat-exchange network involving one-hot, one-cold and one-cooling utility stream (Table 1). For this system, the "input" information is:

$$u = [F_H,\ T_H^{in},\ F_C,\ T_C^{in},\ F_W,\ T_W^{in}]^T \tag{10}$$

and the "output" information is

$$w = [F_H,\ T_H^{out},\ F_C,\ T_C^{out},\ F_W,\ T_W^{out}]^T \tag{11}$$

The IO relations for this system are derived under the assumption of no energy generation of consumption, and are based on the overall energy balance:

$$F_H T_H^{in} + F_C T_C^{in} + F_W T_W^{in} = F_H T_H^{out} + F_C T_C^{out} + F_W T_W^{out} \tag{12}$$

This IO information can be satisfied through several ISO relations. Each ISO relation corresponds to a network structure and can be established based on first principles (for example, the heat balances in all the exchangers).

One particular network and its corresponding state-space representation are shown in Figure 4. The "state" vector is the output of the process operator and input to the distribution network, and can be written as:

$$z = [F_{H1},\ F_{H2},\ T_{H1}^{out},\ T_{H2}^{out},\ F_{C1},\ T_{C1}^{out},\ F_{W1},\ T_{W1}^{out}]^T \tag{13}$$

The "state derivative" vector corresponds to the input of the process operator and is equal to:

$$\dot{z} = [F_{H1},\ F_{H2},\ T_{H1}^{in},\ T_{H2}^{in},\ F_{C1},\ T_{C1}^{in},\ F_{W1},\ T_{W1}^{in}]^T \tag{14}$$

The process operator (•) is such that:

$$z = (\bullet)\dot{z} \tag{15}$$

To mathematically describe this operator one need only specify the heat matches taking place (for example, $H1$-$C1$, $H2$-$W1$), the size of the corresponding exchangers and their describing equations such as:

$$F_{H1} cp_{H1} (T_{H1}^{in} - T_{H1}^{out}) = F_{C1} cp_{C1} (T_{C1}^{out} - T_{C1}^{in}) = U A_{H1,C1} \Delta T \ln_{H1,C1} \tag{16}$$

$$F_{H2} cp_{H2} (T_{H2}^{in} - T_{H2}^{out}) = F_{W1} cp_{W1} (T_{W1}^{out} - T_{W1}^{in}) = U A_{H2,W1} \Delta T \ln_{H2,W1} \tag{17}$$

These equations can indeed be used to determine z from $\dot{z}$. Finally, the particular distribution network employed corresponds to the following realization of the $ABCD$ operator:

$$A = 0 \qquad \dim\ (8 \times 8) \tag{18}$$

$$B = \begin{bmatrix} \frac{F_{H1}}{F_H} & 0 & 0 & 0 & 0 & 0 \\ \frac{F_{H2}}{F_H} & 0 & 0 & 0 & 0 & 0 \\ 0 & 1 & 0 & 0 & 0 & 0 \\ 0 & 1 & 0 & 0 & 0 & 0 \\ 0 & 0 & 1 & 0 & 0 & 0 \\ 0 & 0 & 0 & 1 & 0 & 0 \\ 0 & 0 & 0 & 0 & 1 & 0 \\ 0 & 0 & 0 & 0 & 0 & 1 \end{bmatrix} \tag{19}$$

$$C = \begin{bmatrix} 1 & 1 & 0 & 0 & 0 & 0 & 0 & 0 \\ 0 & 0 & \frac{F_{H1}}{F_H} & \frac{F_{H2}}{F_H} & 0 & 0 & 0 & 0 \\ 0 & 0 & 0 & 0 & 1 & 0 & 0 & 0 \\ 0 & 0 & 0 & 0 & 0 & 1 & 0 & 0 \\ 0 & 0 & 0 & 0 & 0 & 0 & 1 & 0 \\ 0 & 0 & 0 & 0 & 0 & 0 & 0 & 1 \end{bmatrix} \tag{20}$$

$$D = 0 \qquad \dim\ (6 \times 6) \tag{21}$$

As stated earlier, the above-described ABCD and (•) operators give rise to a particular state-space realization of the

Figure 4. Parallel network and its state-space realization corresponding to Table 1.

IO relations. Other state-space realizations of the same IO relations (that is, other process networks fulfilling the same input-output requirements) can be constructed in many other ways. One may consider:

1. A different distribution network (for example, $A \neq 0$)
2. Different exchanger sizes
3. A state vector of higher dimension (for example, 16 rather than 8 giving rise to a network with more units).

One such alternative constitutes a network of exchangers in series as depicted in Figure 5, which has been constructed using the same state-space dimension. The distribution network employed corresponds to the following realization of the *ABCD* operator:

$$A = \begin{bmatrix} 0 & 0 & 0 & 0 & 0 & 0 & 0 & 0 \\ 1 & 0 & 0 & 0 & 0 & 0 & 0 & 0 \\ 0 & 0 & 0 & 0 & 0 & 0 & 0 & 0 \\ 0 & 0 & 1 & 0 & 0 & 0 & 0 & 0 \\ 0 & 0 & 0 & 0 & 0 & 0 & 0 & 0 \\ 0 & 0 & 0 & 0 & 0 & 0 & 0 & 0 \\ 0 & 0 & 0 & 0 & 0 & 0 & 0 & 0 \\ 0 & 0 & 0 & 0 & 0 & 0 & 0 & 0 \end{bmatrix} \tag{22}$$

$$B = \begin{bmatrix} 1 & 0 & 0 & 0 & 0 & 0 \\ 0 & 0 & 0 & 0 & 0 & 0 \\ 0 & 1 & 0 & 0 & 0 & 0 \\ 0 & 0 & 0 & 0 & 0 & 0 \\ 0 & 0 & 1 & 0 & 0 & 0 \\ 0 & 0 & 0 & 1 & 0 & 0 \\ 0 & 0 & 0 & 0 & 1 & 0 \\ 0 & 0 & 0 & 0 & 0 & 1 \end{bmatrix} \tag{23}$$

$$C = \begin{bmatrix} 0 & 1 & 0 & 0 & 0 & 0 & 0 & 0 \\ 0 & 0 & 0 & 1 & 0 & 0 & 0 & 0 \\ 0 & 0 & 0 & 0 & 1 & 0 & 0 & 0 \\ 0 & 0 & 0 & 0 & 0 & 1 & 0 & 0 \\ 0 & 0 & 0 & 0 & 0 & 0 & 1 & 0 \\ 0 & 0 & 0 & 0 & 0 & 0 & 0 & 1 \end{bmatrix} \tag{24}$$

$$D = 0 \qquad (\text{dim } 6 \times 6) \tag{25}$$

One should note that by changing the values of areas in the exchangers, the process operator (•) is altered. Therefore, the process operator (•) is uniquely specified only when its defining equations (based on conservation laws) and the areas and heat-transfer coefficients of the exchangers (parameters of the operator) are specified.

In summary, at the analysis level, the engineer is given the input variables and I-S-O relations (the network and its equations), and is asked to determine the value of the output variables (the outlet temperatures).

Conversely, at the synthesis level, the engineer is given the input and output variables (the input and output flow rates, temperatures, and so on), and is asked to determine the ISO relations (the process network).

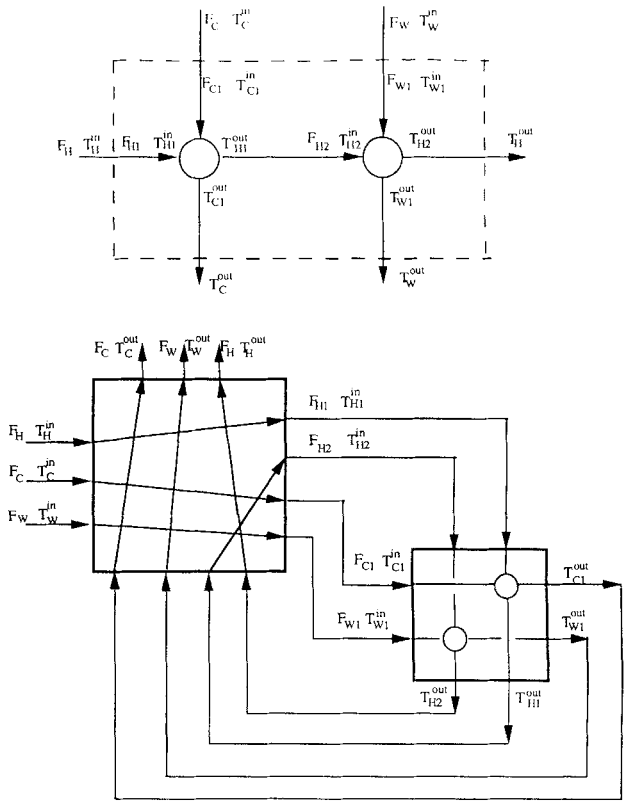

Figure 5. Network in series and its state-space realization corresponding to Table 1.

At the synthesis level, preliminary evaluations, such as the calculation of minimum utility consumption, are often performed. In this case, the engineer is only concerned with the level of utility usage and does not require specific details on the process network itself. This goal is achieved through the so-called "pinch" calculations and leads to another type of process operator termed "the pinch operator." The mathematical description of this and other process operators is provided later.

Distribution Network Mathematical Description. Although exceptions have been suggested (Westerberg, 1989) for the simple case of heat/mass or simultaneous heat- and mass-exchange networks, it is usually assumed that process streams do not mix. Therefore, it is assumed that splitting and mixing in the distribution network take place for streams belonging to different "families." Each family contains all the streams inside the network that emanate from a certain input stream. It is easy to see that in such a case the operators A, B, C, D are *partitioned operators* of the type:

$$A = \begin{bmatrix} A_1 & \cdots & 0 & \cdots & 0 \\ \vdots & \ddots & \vdots & \ddots & \vdots \\ 0 & \cdots & A_i & \cdots & 0 \\ \vdots & \ddots & \vdots & \ddots & \vdots \\ 0 & \cdots & 0 & \cdots & A_n \end{bmatrix} \tag{26}$$

where n is the number of physical streams represented by u and w. The dimensions of the operators of each family depend on the number of "junctions" chosen for that family. The number of junctions, therefore, serves as an upper bound of the number of network streams associated with a certain network input stream.

Operators A_i, B_i, C_i, D_i represent the material and energy balances at the junctions of the DN. Therefore, a complete mathematical description of the DN can be obtained in terms of the splitting ratio of each stream at each DN input junction only.

Finally, the condition of retaining physical identity is a design specification for heat- and mass-exchanger networks where mixing of streams is not allowed. In distillation networks, streams are allowed to mix and split inside the network, so that this design specification is no longer imposed. In this case, one may say that there is only one family and the operators are no longer partitioned.

Superstructure Operator. This operator provides for no mixing and/or splitting, and has the structure of the operators used in Figures 4-5. For each hot/rich stream, only one match with a predetermined cold/lean stream is possible. Each of these matches is *a-priori* parameterized in terms of an integer variable $\eta_{i,j}$ that either allows or disallows heat/mass transfer to take place.

As one utilizes this operator for synthesis purposes, a sufficient number of junctions must be created in the distribution network, so that at least one match between a hot/rich and all cold/lean streams is included. This construction is analogous to the notion of superstructures, as put forth in previous works with various degree of completeness (Sargent and Gaminibandara, 1976; Grossmann and Sargent, 1978; Floudas et al., 1986; Floudas and Ciric, 1989; Yee et al., 1990; Yee and Grossmann, 1990) and leads us to call this operator the "superstructure operator."

The mathematical representation of this operator involves specifying the possible hot-cold matches, the associated energy balances, establishing second thermodynamic law constraints and determining the areas of exchangers. For the example given in Table 1, we created a superstructure operator having two matches. The energy balances and the specification of heat-exchanger areas are given by Eqs. 16-17. The following equations connect the heat load of each match to the integer variable.

$$F_{H1}cp_{H1}(T_{H1}^{\text{in}} - T_{H1}^{\text{out}}) - \Lambda\,\eta_{H1,C1} \le 0 \tag{27}$$

$$F_{H2}cp_{H2}(T_{H2}^{\text{in}} - T_{H2}^{\text{out}}) - \Lambda\,\eta_{H2,W1} \le 0 \tag{28}$$

where Λ is a large number.

To guarantee thermodynamic feasibility, the temperatures involved in each match satisfy the second law of thermodynamics. They are (see Figure 5):

$$T_{C1}^{\text{in}} - T_{H1}^{\text{out}} \le 0 \tag{29}$$

$$T_{C1}^{\text{out}} - T_{H1}^{\text{in}} \le 0 \tag{30}$$

$$T_{W1}^{\text{in}} - T_{H2}^{\text{out}} \le 0 \tag{31}$$

$$T_{W1}^{\text{out}} - T_{H2}^{\text{in}} \le 0 \tag{32}$$

which are complemented with the equations that constrain each stream to be hot and/or cold, respectively:

$$T_{H1}^{\text{out}} \le T_{H1}^{\text{in}} \tag{33}$$

$$T_{H2}^{\text{out}} \le T_{H2}^{\text{in}} \tag{34}$$

$$T_{C1}^{\text{in}} \le T_{C1}^{\text{out}} \tag{35}$$

$$T_{W1}^{\text{in}} \le T_{W1}^{\text{out}} \tag{36}$$

For the case of mass-exchange networks, one needs to use the equilibrium relations to write the second law. Let x_i, $\hat{x}_i$ be the rich-stream inlet and outlet concentrations, and y_j, $\hat{y}_j$ be the inlet and outlet concentrations of the lean stream. Let also $F(x_i)$ be the concentration of a lean stream that is in equilibrium with a rich stream of concentration x_i. Assume further that $F(x) > x$, that is, $F(x)$ is concave. There is no loss in generality in this assumption, since one can always replace the convex portion of the equilibrium function with piecewise linear approximations. Then, for the case of mass exchange, the second law (feasibility) is satisfied if:

$$\hat{y}_j - F(x_i) \le 0 \tag{37}$$

$$y_j - F(\hat{x}_i) \le 0 \tag{38}$$

If one wishes to pursue to solution of a network synthesis problem featuring minimum total annualized cost using this operator, then the corresponding objective function has the structure:

$$c_W F_W + [\eta_{H1-C1}(\beta + \alpha A_{H1-C1}^{\gamma}) + \eta_{H2-W1}(\beta + \alpha A_{H2-W1}^{\gamma})] \tag{39}$$

where c_W, α, β, and γ are the cost parameters.

The dimensionality of the problem posed by the mathematical description of this operator often exceeds the capabilities of known optimizers, even for the pure HEN or MEN design cases in which each pair of streams are allowed to match only once throughout the network (acyclic networks). It is, therefore, imperative to turn our attention to other operators that can be computationally more amenable. A large variety of other operators can be conceived, in response to a particular network synthesis problem's characteristics. Next we outline some of these.

Assignment Operator. This operator is similar to the superstructure operator in that it also does not allow stream splitting and/or mixing. Each stream is matched only once but the hot-cold matches are not specified *a priori*. Instead, it is assumed that any hot stream may match with any cold stream though each stream may be matched only once. The structure of this operator is depicted in Figure 6. This flexibility is parameterized in terms of the integer variables $\eta_{i,j}$ associated with each hot i-cold j match. These variables satisfy the assignment constraints:

$$\sum_i \eta_{i,j} = 1 \tag{40}$$

$$\sum_j \eta_{i,j} = 1 \tag{41}$$

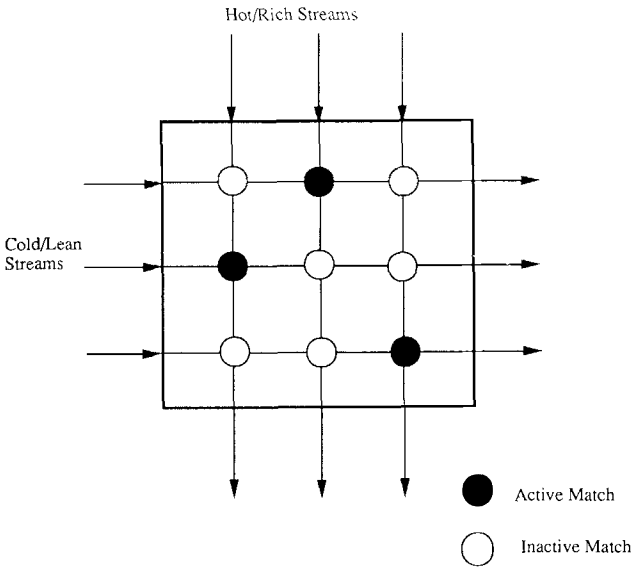

Figure 6. Assignment operator.

The resulting optimization problem features the property of the "assignment problem in linear programming" to naturally possess integer solutions for $\eta_{i,j}$. Therefore, the overall network's optimization could be pursued with NLP rather than MINLP solvers.

The mathematical statement of this operator is identical to that of the superstructure operator, except for the additional assignment constraints (Eqs. 40-41). Additionally, one has to multiply each feasibility constraint by $\eta_{i,j}$ so that only the active match is forced to be feasible.

The particular structure of this operator may allow the solution of a particular network synthesis problem with less junctions than the superstructure operator.

Pinch Operator. This operator specifies the amount of heat/mass to be taken away from an incoming hot/rich stream, and the amount of heat/mass to be given to an incoming cold/lean stream. In doing so it uniquely determines the exit temperatures for each of these streams and thus the state of the overall process network.

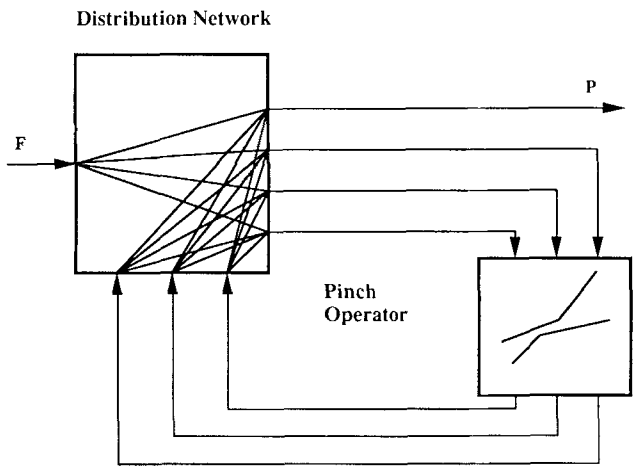

Figure 7. State-space realization of a HEN (MEN) network using the pinch operator.

Although minimum utility usage for HEN or MEN alone can be calculated without the use of the state-space approach, this cannot be done for interacting HEN and MEN. Nevertheless, to present the operator, we restrict ourselves to the case of HEN or MEN alone (Figure 7).

The operator's definition requires that these amounts of heat/mass be acquired or be taken away in agreement with the first and second laws of thermodynamics. Employing a temperature/concentration heat/mass load diagram one can enforce these laws as follows.

First law:

$$\left\{\begin{matrix}\text{heat/mass lost}\\ \text{by hot/rich streams}\end{matrix}\right\} - \left\{\begin{matrix}\text{heat/mass gained}\\ \text{by cold/lean streams}\end{matrix}\right\} = 0 \quad (42)$$

Second law:

$$\left\{\begin{matrix}\text{The composite hot/rich stream should}\\ \text{lie above the composite cold/lean stream}\end{matrix}\right\} \quad (43)$$

Based on the results of Grimes (1980), Cerda et al. (1983), and Duran and Grossmann (1986) for HEN and El-Halwagi and Manousiouthakis (1990a,b) for MEN, the latter condition need be enforced only at the inlet temperatures/concentrations of each stream (the so-called "pinch point candidates"). Therefore, the second law can be restated as:

$$\left\{\begin{matrix}\text{heat/mass lost by hot/}\\ \text{reach streams below the}\\ \text{pinch point candidate}\end{matrix}\right\} - \left\{\begin{matrix}\text{heat/mass gained by cold/}\\ \text{lean streams below the}\\ \text{pinch point candidate}\end{matrix}\right\} \leq 0 \quad (44)$$

for all pinch point candidates.

The exact representation of the pinch operator for our example is:

First law:

$$F_{H1}cp_{H1}(T_{H1}^{in} - T_{H1}^{out}) + F_{H2}cp_{H2}(T_{H2}^{in} - T_{H2}^{out}) = F_{C1}cp_{C1}(T_{C1}^{out} - T_{C1}^{in}) + F_{W1}cp_{W1}(T_{W1}^{out} - T_{W1}^{in}). \quad (45)$$

Second law:

In the mathematical representation of the pinch inequalities one must take into account only the portion of load that corresponds to all the temperatures below the pinch candidate. This is easily done when the operator's inlet and outlet temperatures are known. However, since these are now variables, one must incorporate into the mathematical description variables that would recognize the relative values of these temperatures with respect to the pinch candidate. For example, for the pinch candidate T_{H1}^{in} we introduce:

$$s_{H2-H1}^{in} = \text{Max}\{T_{H2}^{in}, T_{H1}^{in}\} \quad (46)$$

$$s_{H2-H1}^{out} = \text{Max}\{T_{H2}^{out}, T_{H1}^{in}\} \quad (47)$$

$$r^{in}_{C1-H1} = \text{Max}\{T^{in}_{C1},\ T^{in}_{H1} - \Delta T\} \quad (48)$$

$$r^{out}_{C1-H1} = \text{Max}\{T^{out}_{C1},\ T^{in}_{H1} - \Delta T\} \quad (49)$$

$$r^{in}_{W1-H1} = \text{Max}\{T^{in}_{W1},\ T^{in}_{H1} - \Delta T\} \quad (50)$$

$$r^{out}_{W1-H1} = \text{Max}\{T^{out}_{W1},\ T^{in}_{H1} - \Delta T\} \quad (51)$$

where the minimum approach temperature difference ΔT was used.

Then the pinch inequality for this pinch candidate is, therefore, written as follows:

$$F_{H1}cp_{H1}(T^{in}_{H1} - T^{out}_{H1}) + F_{H2}cp_{H2}[(T^{in}_{H2} - s^{in}_{H2-H1}) - (T^{out}_{H2} - s^{out}_{H2-H1})] - F_{C1}cp_{C1}[(T^{out}_{C1} - r^{out}_{C1-H1}) - (T^{in}_{C1} - r^{in}_{C1-H1})] - F_{W1}cp_{W1}[(T^{out}_{W1} - r^{out}_{W1-H1}) - (T^{in}_{W1} - r^{in}_{W1-H1})] \le 0 \quad (52)$$

Similar equations can be written for the other pinch candidates T^{in}_{H2}, T^{in}_{C1}, and T^{in}_{W1}.

Stream self-recycles have been included as part of the DN flows. Stream self-recycles are defined as distribution network flows connecting the inlet and outlet of the DN for the same stream. When these recycles are present in streams that pass through only one pinch operator, they can be eliminated without violating the second-law thermodynamic requirements associated with the pinch operator.

Indeed, consider a hot/rich stream that passes through a pinch operator and presents a self-recycle, as shown in Figure 8. If one maintains the temperature/concentration at the outlet of the pinch operator fixed and eliminates the self-recycle, then as the heat/mass released by this stream must remain the same (because of the first thermodynamic law requirements), the temperature/concentration at the inlet of the pinch operator increases. The composite hot/rich stream of the pinch operator will, therefore, be altered showing an increase in the corner corresponding to this stream's inlet temperature/concentration. As inlets of streams are pinch point candidates, the second thermodynamic law requirements can only be made easier to satisfy. In Figure 9, a typical unpinched solution of a minimum utility problem is depicted in terms of the final composite curve diagrams. No self-recycles are included in this solution. Suppose now that the self-recycle on stream C_2 is increased. The new stream $\hat{C}_2$ will have greater flow rate and initial temperature. A simple energy balance reveals that the new initial temperature will be such that the heat load is the same as for C_2. The resulting composite curve will be risen creating a pinch point. Further increase of the recycle will violate the second law. Since the amount of heat transferred does not change, no changes in the utility consumption are observed in increasing the recycle. Conversely, if the solution had contained a recycle for stream C_2, this recycle can be eliminated, since the slope would be reduced, and thus the cold composite curve would lie farther away from the hot stream.

It can be summarized that a state-space model that uses pinch operators, can be constructed omitting the stream self-recycles around each pinch operator. Other recycles inside the DN should, however, remain intact to capture all possible solutions.

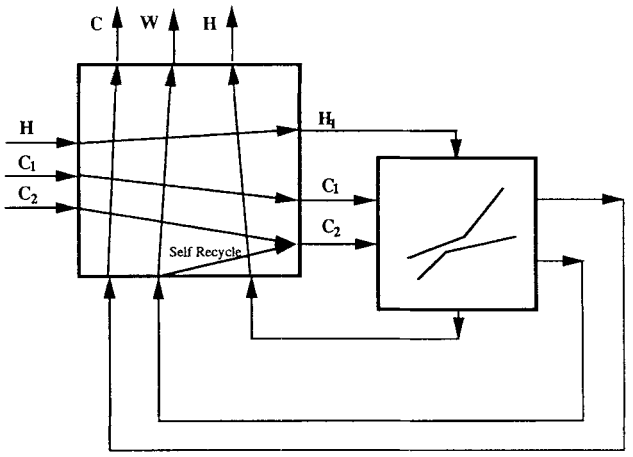

Figure 8. Self-recycle on a pinch operator.

It should be emphasized that the use of the pinch operator becomes of paramount importance only in the case of HEN/MEN interacting, either with one another or with other process operators. In the following sections we demonstrate that this is exactly what happens in distillation networks.

Split-Matching Operator. This operator allows both stream splitting and mixing. Every hot/rich stream entering the operator is split into as many streams as cold/lean streams present. Similarly, every cold/lean stream (including utility streams) are split into as many streams as hot/rich streams present. Then, one hot/rich-cold/lean match is created for each resulting stream as shown in Figure 10. Several options may be pursued in further defining this operator. For example, one may assume that the operator's internal streams that mix with one another all have the same temperature. This assumption allows the thermodynamic feasibility of each match to be assessed based on the operator's input and output information.

For our example, let Q_{H1-C1}, Q_{H1-W1}, Q_{H2-C1} and Q_{H2-W1} be the heat exchanged in each match. The first law of thermodynamics is satisfied if:

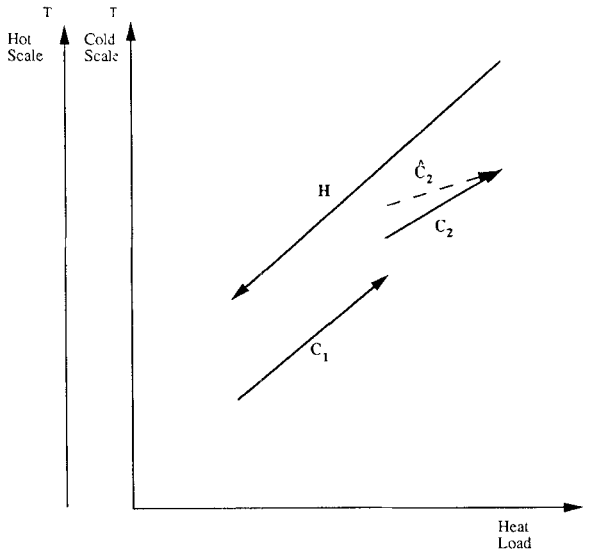

Figure 9. Effect of self-recycles on the temperature-heat load diagram.

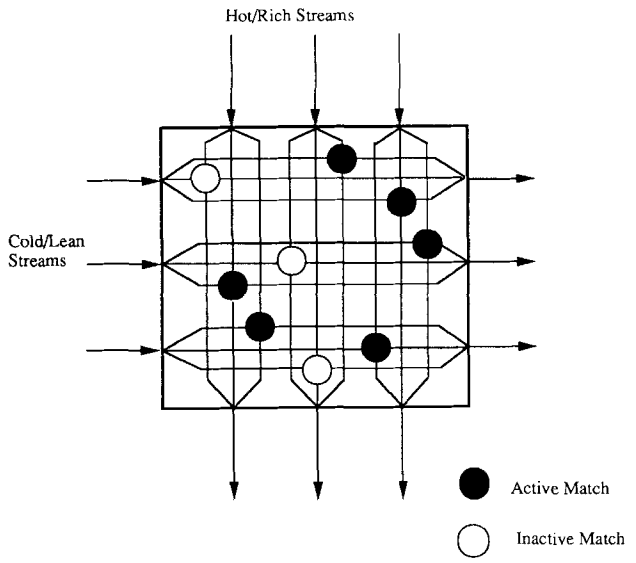

Figure 10. Split-matching operator.

$$F_{H1}cp_{H1}(T_{H1}^{in}-T_{H1}^{out})=Q_{H1-C1}+Q_{H1-W1} \quad (53)$$

$$F_{H2}cp_{H2}(T_{H2}^{in}-T_{H2}^{out})=Q_{H2-C1}+Q_{H2-W1} \quad (54)$$

$$F_{C1}cp_{C1}(T_{C1}^{out}-T_{C1}^{in})=Q_{H1-C1}+Q_{H2-C1} \quad (55)$$

$$F_{W1}cp_{W1}(T_{W1}^{out}-T_{W1}^{in})=Q_{H1-W1}+Q_{H2-W1} \quad (56)$$

In the context of minimum utility calculations, one requires that each active match satisfy the second law, within a tolerance given by ΔT. For our example, this is written as:

$$Q_{H1-C1}(T_{C1}^{out}+\Delta T-T_{H1}^{in})\le 0 \quad (57)$$

$$Q_{H1-C1}(T_{C1}^{in}+\Delta T-T_{H1}^{out})\le 0 \quad (58)$$

$$Q_{H1-W1}(T_{W1}^{out}+\Delta T-T_{H1}^{in})\le 0 \quad (59)$$

$$Q_{H1-W1}(T_{W1}^{in}+\Delta T-T_{H1}^{out})\le 0 \quad (60)$$

$$Q_{H2-C1}(T_{C1}^{out}+\Delta T-T_{H2}^{in})\le 0 \quad (61)$$

$$Q_{H2-C1}(T_{C1}^{in}+\Delta T-T_{H2}^{out})\le 0 \quad (62)$$

$$Q_{H2-W1}(T_{W1}^{out}+\Delta T-T_{H2}^{in})\le 0 \quad (63)$$

$$Q_{H2-W1}(T_{W1}^{in}+\Delta T-T_{H2}^{out})\le 0 \quad (64)$$

Table 2. Heat Exchange Network Stream Data (One-Hot, One-Cold and Two Utility Streams)

Stream	Flow (kg/s)	T_{in} (°C)	T_{out} (°C)
H	1	100	40
C	2	70	90
W	—	15	35
S	—	110	110

cp = 4.184 kJ/kg·°C; minimum approach temp. = 5°C

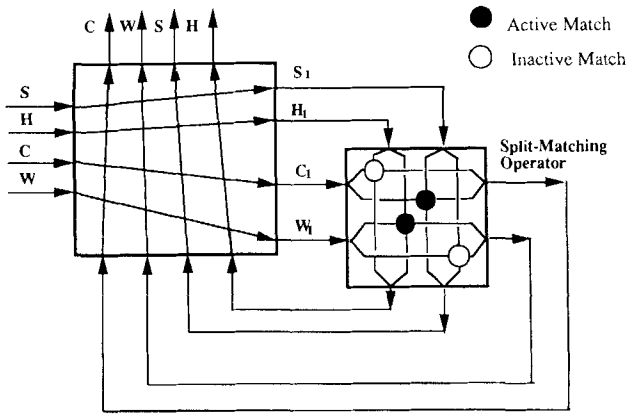

Figure 11. State-space realization of the HEN corresponding to Table 2 using a split-matching operator with one junction per stream.

For mass-exchanger networks, one introduces a minimum approach ϵ and requires that:

$$Q_{i,j}[\hat{y}_j+\epsilon-F(x_i)]\le 0 \quad (65)$$

$$Q_{i,j}[y_j+\epsilon-F(\hat{x}_i)]\le 0 \quad (66)$$

As in the pinch operator, the utility demand is given by the values of the heat transferred to or from the utility streams.

When minimizing utility cost, the split-matching operator can provide the same minimum utility predicted by the pinch operator, provided enough junctions are allowed in the DN. Indeed, when the second-law temperature inequalities (before being multiplied by the heat transferred) are both simultaneously satisfied, the $i-j$ match is *feasible* and the amount of heat/mass that can be exchanged between stream i and j is limited only by the lowest of the loads. When only one of these inequalities is satisfied, the match is *partially infeasible*. Finally, when both inequalities are violated, the match is *totally infeasible*.

In the absence of partially feasible matches, the solution obtained using the split-matching operator is the same as that obtained using the pinch operator. This is so because all feasible heat/mass transfer can be realized. On the other hand, as enough junctions are provided, any partially feasible match can be transformed into one feasible and one totally infeasible match. As a result, the minimum utility predictions of the pinch operator can be exactly realized.

Let us illustrate this with an example. Consider the case of Table 2. The solution obtained when only one junction per stream is used is depicted in Figure 11. This solution corresponds to a network where stream H is cooled using cooling utility and stream C is heated using steam. It is because both streams have to exchange all their required heat using only one stream in the operators. With this amount of junctions, this particular state space cannot realize the real minimum utility. In this particular solution, it is possible to identify one partially feasible match. It corresponds to the match $H1-C1$. Therefore, we conclude that the solution obtained cannot possibly be a minimum utility solution. Indeed, if we add one more junction to the family corresponding to stream H, one can realize the minimum utility, as depicted in Figure 12.

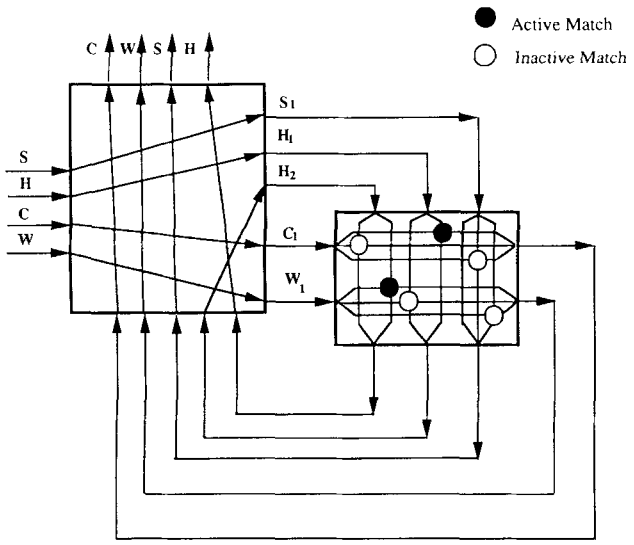

Figure 12. State-space realization of the HEN corresponding to Table 2 using a split-matching operator with two junctions per stream.

Block-Partitioned Operators. Consider the case in which both heat and mass need to be exchanged between a given set of streams (the supply temperatures and concentrations differ from the target temperatures and concentrations). It is known that pinch or split-matching calculations can be done for the case of heat exchange or isothermal mass exchange alone. But can they be performed when both commodities are exchanged within the network? To answer this question, we consider two forms of heat/mass exchange that can take place inside a heat/mass exchange network.

• When heat and mass exchange take place within the same unit, its heat/mass transfer is called *simultaneous*.

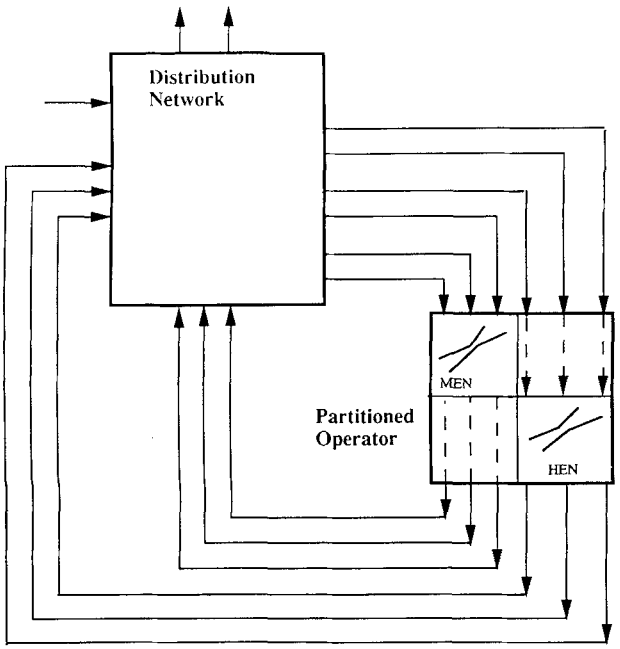

Figure 13. State-space realization of a HEN (MEN) using block-partitioned pinch operators.

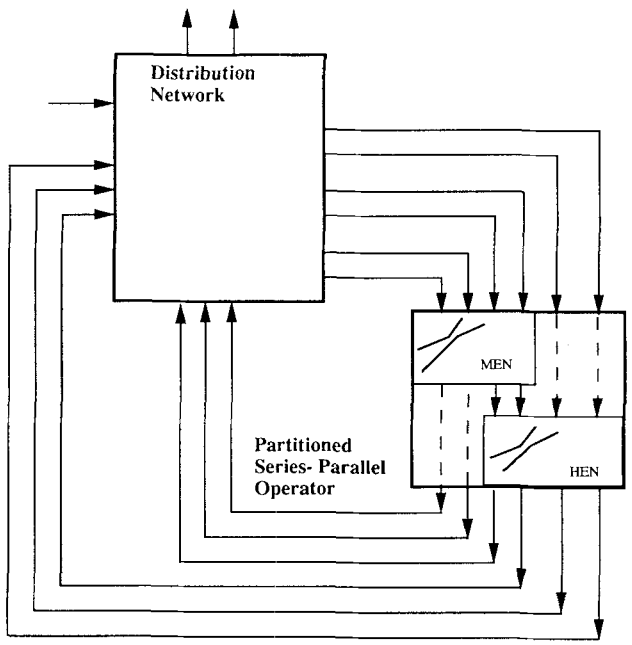

Figure 14. State-space realization of a HEN (MEN) using block partitioned parallel-series pinch operators.

• When heat and mass exchange take place within the network but in different units, its heat/mass transfer is called *separable*.

In the case of separable heat/mass exchange, the above-mentioned pinch or split-matching operators can be used to calculate minimum utility cost within the state-space framework. The necessity of the state-space framework stems from the inability to construct temperature interval diagrams (TID) and concentration interval diagrams (CID), as there is no *a-*

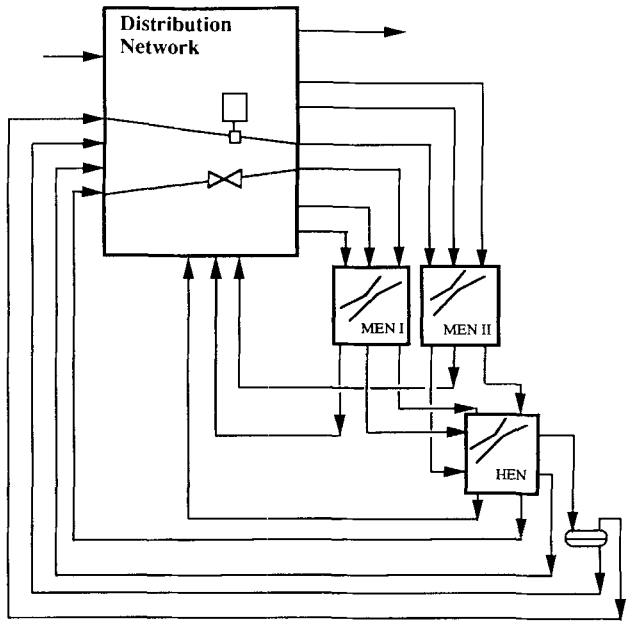

Figure 15. State-space realization of a separable MEN-HEN with two MENs at different pressures.

priori knowledge of the inlet and outlet temperatures and compositions of the streams participating in the HEN and MEN. There is indeed a trade-off between mass-separating agent and heating-cooling costs; as a result, an optimization procedure is required to determine the level or levels of temperature at which mass transfer should take place. Figure 13 shows how the different mass-pinch and heat-pinch assessments can be realized by a partitioned pinch operator.

Series operations of such type as *mass exchange-heat exchange* require one stream with only one inlet and one outlet junction in the distribution network *per each operation*. If these series operations are allowed to be performed within the operator, as shown in Figure 14, only one stream will be used, with the resulting reduction of dimensionality.

Auxiliary Operators. Distillation includes phase separation and is therefore desirable that isobaric and adiabatic flash separation be represented within the state-space framework. For this purpose, a phase separation operator can be defined for each stream at the outlet of the HEN and before it is introduced into the DN.

As one may allow pressure changes in the network, an operator that performs compression or expansion, allowing the addition of mechanical energy and the adiabatic expansion of streams, is also introduced. This can be done outside the DN for each stream or even be considered inside the distribution network associated with the DN internal streams. The advantage of allowing pressure changes inside the distribution network is that the number of possibilities increases. For example, one may split one stream, and compress or expand each of the splits separately. Since streams going to the MEN have to be at the same pressure, MENs at different pressure levels need to be defined. Figure 15 shows the complete parallel-series operators with two MEN operating at different pressures.

Distillation Networks as Heat- and Mass-Exchange Networks

A conventional distillation column can be viewed as a composite heat- and mass-exchanger operation. As shown in Figure 16, two mass exchangers and two heat exchangers are needed to create the small network that represents a conventional distillation column with a two-phase feed stream. Its state-space realization is shown in Figure 17.

Two exchange operations take place inside a distillation network. On one hand, pure heat-transfer operations take place in condensers, reboilers, preheaters, and so on. On the other hand, simultaneous heat and mass transfers take place inside the columns.

One of the major difficulties in analyzing the problem using MEN and HEN tools is that the intermediate streams inside the network are not known in advance and have to be generated during the design procedure. Once this is accomplished, heat and mass integration among the different streams can be analyzed using classical HEN and MEN approaches embedded in the overall design procedure.

Assuming constant countercurrent molar flow rate, mass exchange inside distillation columns, though nonisothermal, can be treated as a pure mass-transfer operation. This is the basis of the McCabe-Thiele method. In this case, a distillation network can be considered as a separable heat/mass-exchange network.

The other distinctive feature of the distillation network is

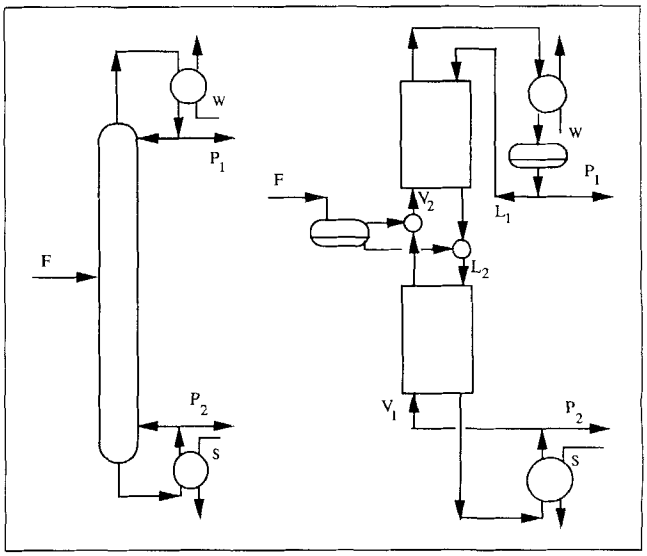

Figure 16. Distillation as a composite heat/mass exchanger network: column with two-phase feed.

that streams are allowed to mix and split, so that they lose their identity as soon as they enter the distribution network.

In this particular state-space realization of a distillation network, different combinations of operators can be used. Split-matching or pinch operators can be used for mass exchange and heat exchange depending on designer preferences.

More complicated networks can be represented in this way. A Petlyuk arrangement with liquid feed and liquid products is represented in Figure 18. Its state-space realization is shown in Figure 19, where only active matches in the split-matching operator are shown. Another interesting feature of this state-space realization is that an independent circuit can be established for a heat pump, as shown in Figure 20.

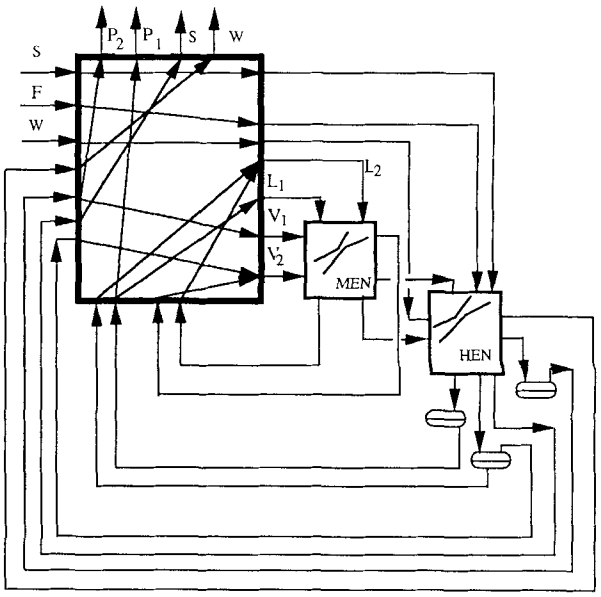

Figure 17. State-space realization of a single column with a two-phase feed.

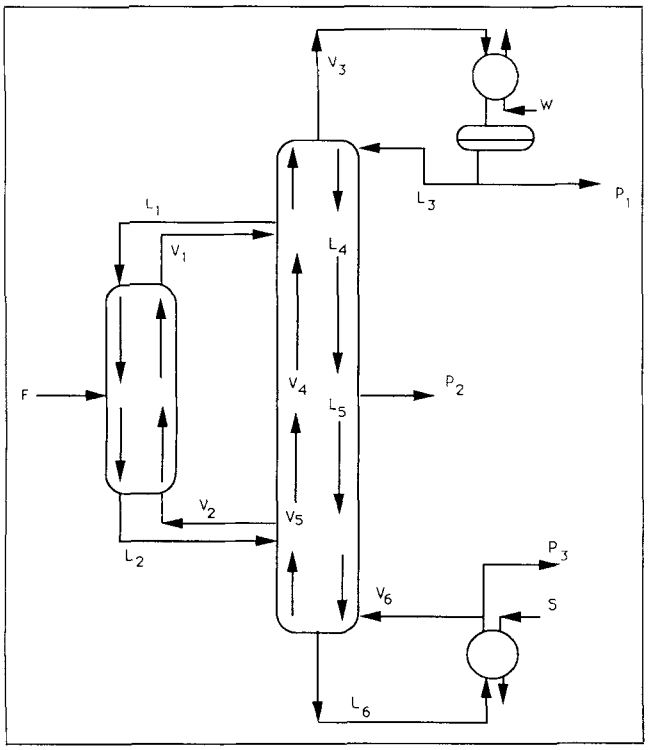

Figure 18. Conventional representation of a Petlyuk column.

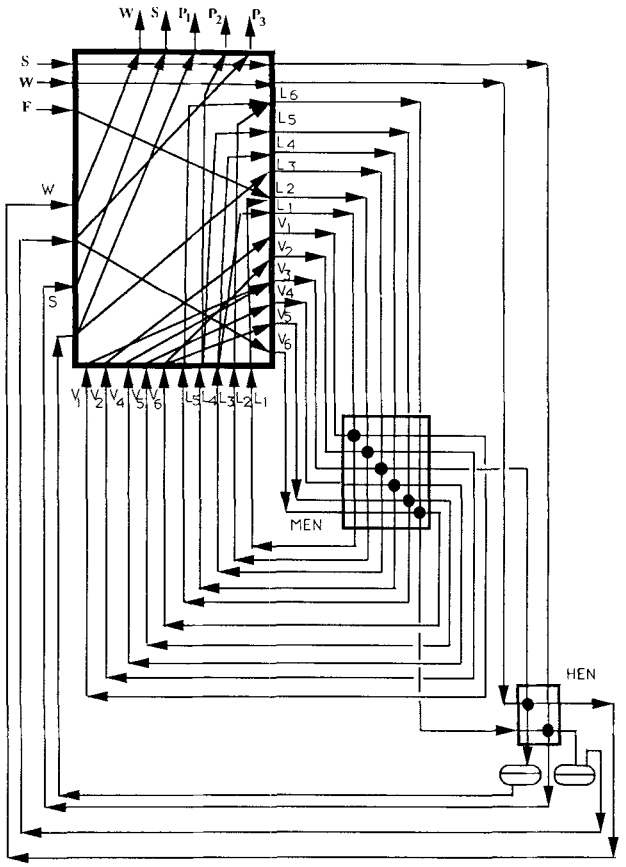

Figure 19. State-space realization of a Petlyuk column using a split-matching operator.

Only active matches are shown.

Assumptions

To perform the design of energy-efficient distillation networks with multiple feed and multiple product streams, the following assumptions are made:

(a) Target compositions for the separation task are given for only one component, which is called the "key" component.

(b) For heat/mass-exchange operations, only distillation-type (vapor-liquid) mass exchangers are to be considered as part of the network.

(c) Thermodynamic equilibrium properties of the key species are not a function of the composition of other species.

(d) Enthalpy of vapor and liquid mixtures can be expressed as a function of the temperature, pressure and composition of the key component.

(e) Only countercurrent contact in mass exchangers between liquid and vapor streams are considered. Constant molar flow rate is assumed to hold for both streams, and each equilibrium stage is 100% efficient.

(f) No mass separating agent is used.

(g) Different pressure levels are fixed.

(h) An independent circuit for a heat pump can be used.

We should emphasize that the state-space approach can be applied to *any* distillation network synthesis problem, irrespective of the validity of these assumptions. Nevertheless, in the interest of simplicity of presentation and as a first attempt to the general problem description, we have chosen to limit the scope of this work to problems satisfying these assumptions.

Assumptions a, c and d trivially hold true for binary mixtures. They are also the basis of the key component approach to multicomponent distillation.

Although other technologies (such as mass-separating agents) can be considered at the same time within the state-space approach, assumption b is included only for simplicity.

Assumption c holds for ideal multicomponent mixtures. Mixtures of nonpolar compounds of similar structure and molecular weight satisfy this assumption fairly well. This assumption was used extensively in the modeling of multicomponent distillation (Holland, 1981) of mixtures of aliphatic or aromatic hydrocarbons of similar molecular weight (especially isomers).

For ideal mixtures, assumption d is a good approximation when the enthalpies of pure components are close.

Finally, assumption e implies that energy balances around distillation columns are ignored. This is similar to the well known assumption of the McCabe Thiele method for distillation column design.

Since mass transfer is equilibrium-driven (assumption e), the temperatures and enthalpies of the streams leaving the MEN are those corresponding to saturated liquid and vapors.

Details of the state-space model in its complete mathematical form as applied to this particular problem are given in the Appendix.

MEN and HEN Interactions

In this section, the background provided by the state-space realization of distillation networks is used to analyze the in-

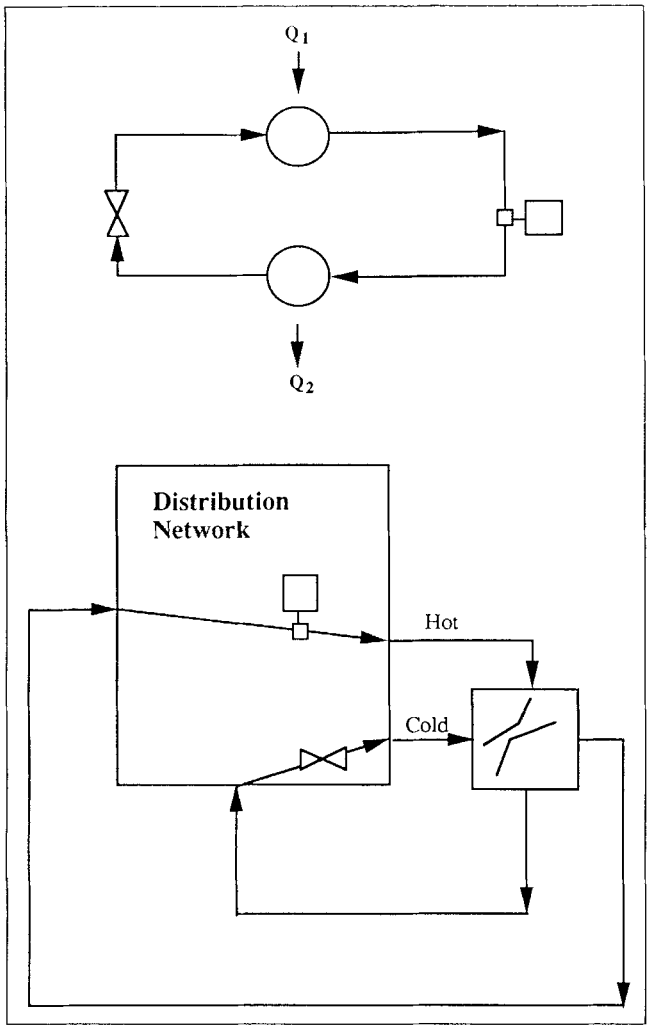

Figure 20. State-space realization of an external heat pump circuit.

teraction between the corresponding MEN and HEN through the DN. First, simple distillation column designs obtained using the McCabe-Thiele method are discussed. Next, two-column multieffect-type designs are analyzed. Finally, a two-feed, two-product solvent-water separation system is discussed.

Analysis of single distillation column

We will first illustrate how the information outlined in the familiar McCabe-Thiele diagram can be represented through HEN/MEN pinch diagrams and how this novel representation can be used to analyze conventional designs. Although the discussion that follows is limited to a single distillation column, one of the primary advantages of the MEN/HEN pinch diagrams is that they can be used to represent information regarding a whole network, something that conventional McCabe-Thiele diagrams cannot do. Networks involving more columns cannot be easily analyzed and/or designed using the McCabe-Thiele method, which does not take into account the possibilities of heat integration and multiple columns. Therefore, the knowledge and understanding of the MEN/HEN

Table 3. Data for the Propane-Propylene Splitting Case Study

Feed	271.8	kmol/h	$z=0.6$	$T=362$ K	$P=106$ psia
Products	159.0	kmol/h	$w=0.99$	@Sat. Vapor	$P=106$ psia
	112.8	kmol/h	$w=0.05$	@Sat. Vapor	$P=106$ psia
Costs:					
Steam		$1.6/1,000 lb			$=\$\ 1.7515/10^6$ kJ
Cooling Water		$0.08/1,000 gal (40°F rise)			$=\$\ 0.2572/10^6$ kJ
Electricity		$0.04/kWh			$=\$12.3646/10^6$ kJ
(Cooling Water is available at 65°F)					

SI conversion: kPa = psi × 6.89; kg = lb × 0.454; °C = (°F − 32)/1.8; MJ = kWh = 3.60.

interactions gained with the analysis of this simple one-column case can be later used for more complicated systems.

For the purpose of illustrating the interaction between the MEN and the HEN networks, a propane-propylene separation (C3 splitting) case study has been chosen.

Every year over 20 million metric tons of polypropylene are produced from propane. Distillation is the method the chemical industry usually employs to separate propane from propylene, and a substantial amount of energy is involved in the process. The incentive to improve the energy efficiency of this separation task is great, and the problem has received the attention of various authors (Tyreus and Luyben, 1975; Finelt, 1979; Quadri, 1981).

The properties of the feed and product streams as well as relevant cost coefficients are given in Table 3. A few words about the thermodynamics of this system are pertinent at this point. The mixtures can be treated as ideal solutions, and both species have very close boiling points. Therefore, their separation using distillation is energy- and capital-intensive. Both effects are related to the fact that the equilibrium line in a y-x diagram is close to the 45° line.

If the separation is conducted at the same pressure as that of the feed and product streams [106 psia (730 kPa)], a refrigerant must be used because of the low dew point of the mixture [the boiling point of propane at 106 psia (730 kPa) is 287.81 K]. The refrigerant cycle chosen uses propane betwen 72 and 230 psi (496 and 1,585 kPa), and its final cost is of $\$2.96/10^6$ kJ.

Assume that the McCabe-Thiele method is used to design a single distillation column. Figure 21 shows the flowsheet of such a distillation column in the form of a mass/heat-exchanger network, employing a partial condenser and a total reboiler.

One of the assumptions of the McCabe-Thiele method is that streams inside each column section have constant molar flow rates. As a result, the two operating curves, corresponding to the two mass exchangers, are straight lines in a y-x diagram (Figure 22). The following facts are also well established in the literature (McCabe et al., 1985):

- The operating line corresponding to the lower mass exchanger has its lower end $(\hat{x}_2, y_1)$ at the 45° line and has a slope of L_2/V_1.
- The operating line corresponding to the upper mass exchanger has its upper end point at $(x_1, \hat{y}_2)$. Its interception with the 45° line is (w_1, w_1) and its slope is $L_1/V_2 = R/(R+1)$, where R is the reflux ratio $\{R = L_1/P_1\}$.
- The two operating lines intersect at a point that lies on

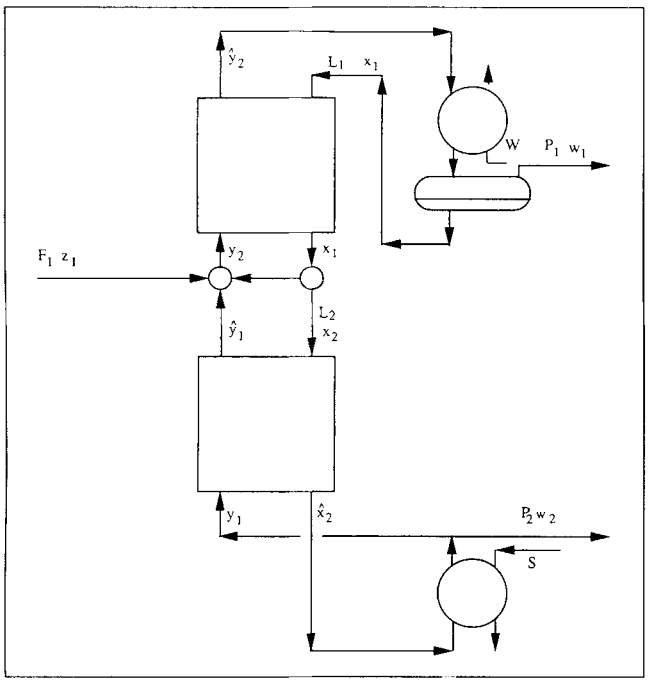

Figure 21. Heat- and mass-exchange network for a distillation column with superheated feed.

the "feed line." In turn, the "feed" line has slope $q/(q-1)$, where q is the parameter describing the phase state of the feed stream.

- The optimal location of the feed plate is the one that straddles the intersection point of the two operating lines. For a given reflux ratio, placement of the feed at any other location results in an increase in the number of plates.
- As the reflux ratio decreases, L_1, L_2, V_1 and V_2 decrease, the condenser and reboiler loads (which are proportional to V_2 and L_2) decrease, and the number of plates increases.

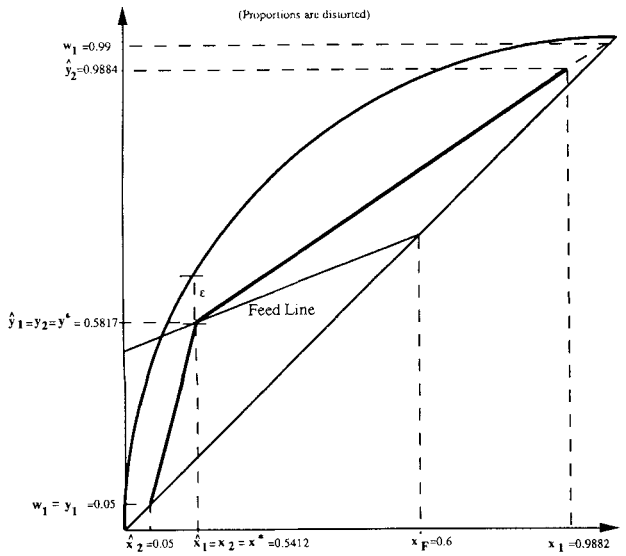

Figure 22. McCabe-Thiele diagram for the C3 distillation column.

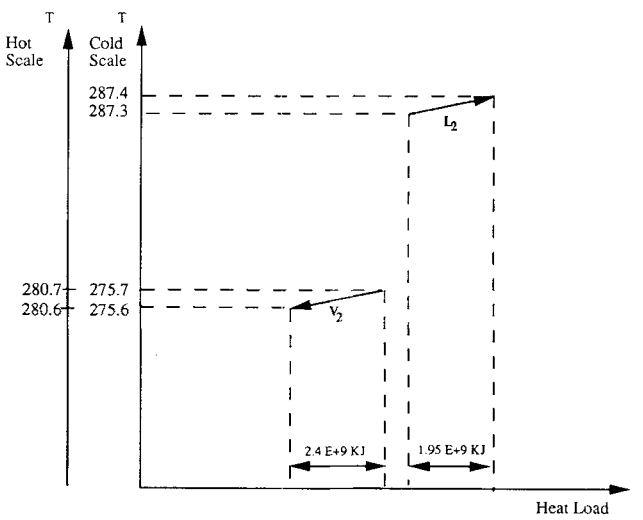

Figure 23. Pinch diagram for the C3 problem.

Let us now describe in detail how the HEN temperature-heat load (T-HL) and the MEN concentration-mass load (C-ML) pinch diagrams are built. For the case of HEN, the task is straightforward, as shown in Figure 23. To ensure finite heat exchange area, it is necessary that a driving force of at least ΔT be maintained between hot and cold streams. Thus, in creating the T-HL diagram, different temperature scales are employed for hot and cold streams. The cold stream temperature scale is chosen to be linear, while the hot stream temperature scale is chosen as a downward translation of the cold scale by an amount ΔT. Thermodynamic feasibility of heat exchange is then maintained as long as the hot composite stream lies above the cold composite stream in the T-HL pinch diagram. Streams in the T-HL diagram are straight lines because their flow rate and heat capacity are assumed to be constant. The slope of these lines is the inverse of the flow rate times heat capacity product. As a result, the composite hot and cold streams are piecewise linear, and pinch points can be easily identified by determining the places in which composite streams touch. Moreover, the only temperature values that are pinch-point candidates are inlet temperatures of hot and cold streams (Grimes, 1980; Cerda et al., 1983; Duran and Grossmann, 1986).

Since the temperature of the condenser is lower than that of the reboiler, the cold stream L_2 is located higher than the hot stream V_2 in the T-HL diagram, demonstrating no possibility of heat integration. This is immediately apparent within the MEN/HEN representation which also provides the necessary utility loads. This information is not directly representable on the McCabe-Thiele diagram.

Construction of the C-ML pinch diagram requires first the selection of corresponding scales for rich and lean streams. These scales should be such that thermodynamic feasibility of mass exchange can be easily assessed through simple inspection of the C-ML pinch diagram. Furthermore, they should incorporate information regarding a minimum driving force ϵ required to keep mass exchangers at finite size. Thermodynamic feasibility of mass exchange is established when both ends of a mass exchanger's operating line lie below the equilibrium curve (or above if the equilibrium curve is based on the heavier component) in a y-x diagram. The distance of these points to

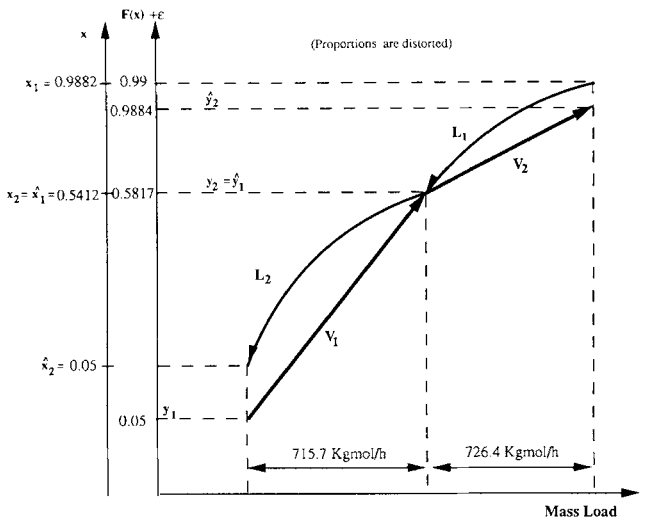

Figure 24. MEN pinch diagram for the C3 problem.

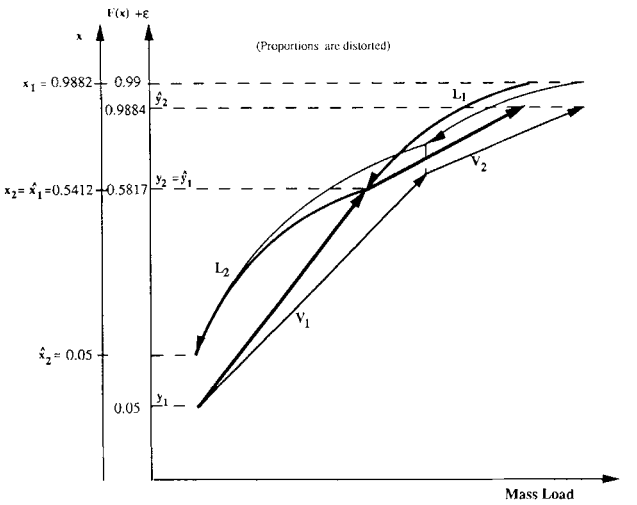

Figure 25. Effect of changes of reflux ratio on the MEN pinch diagram.

the equilibrium curve, therefore, represents the driving force for mass exchange. This suggests that the correspondence of the vapor (lean in the light component) concentration scale and the liquid (rich in the light component) concentration scale should be established through the equilibrium expression $F(x)$. For example, a rich stream with concentration x can exchange mass with a lean stream of concentration y, only if $y \leq F(x) - \epsilon$. For a given linear vapor (lean) concentration scale y, the liquid (rich) concentration scale can be obtained using the transformation $G(y+\epsilon)$, where $G(y)$ is the inverse of $F(x)$. The resulting scale correspondence for the C3-splitting problem is shown in Figure 24.

The McCabe-Thiele assumption of constant molar flow rate suggests that the vapor streams are represented as straight lines in a C-ML pinch diagram with a linear vapor (lean) concentration scale. The slope of these lines is equal to the inverse of the molar flow rate. In their own linear concentration scale, liquid (rich) streams are also represented as straight lines. However, since the mapping $G(y+\epsilon)$ is employed in constructing the liquid (rich) concentration scale, the liquid streams have a curved representation in the C-ML diagram. Fortunately, since $F(x)$ is a nonlinear concave function, the liquid streams are represented by concave curves. As a result, thermodynamic feasibility of mass exchange can be verified through the examination of stream end point information alone. Moreover, the rich composite stream will consist of concave sections. This can be easily seen if one constructs first the composite-rich stream in its own linear scale x and then employs the transformation. Therefore, a pinch analysis can still be performed according to the rule originally proposed by Grimes (1980) for HEN and modified accordingly for MEN by El-Halwagi and Manousiouthakis (1990a): that is, only the inlet concentrations of the rich and lean streams are pinch-point candidates. Thus, for all practical purposes, the piecewise concave composite-rich stream created above can be replaced by a piecewise linear composite-rich stream, without introducing any error in pinch calculations. For this reason, the straight line representation is used from now on.

For the example of the C3-splitter (Figure 24), construction of the composite curves in the C-ML diagram is straightforward because:

- The required product specifications uniquely determine the concentrations $\hat{x}_2$, y_1 and x_1.
- Flow rates are known, once the reflux ratio is fixed.
- The outlet composition of V_1 and L_1 are equal to the inlet compositions of V_2 and L_2, respectively. In the case of the liquid streams, this is true because the outlet of the upper mass exchanger does not mix with any other stream. In the case of the vapor streams, the equality of compositions is related to the fact that the feed plate straddles the intersection of the operating lines in the y-x diagram.

The primary goal in designing energy-efficient distillation networks is to reduce the utility consumption in the HEN. Since in the design under consideration the feed stream is introduced directly to the column, no heat integration is possible and the above goal is translated simply into the goal of reducing the flow rates of L_2 and V_2. Changes in flow rates affect the MEN as well, and thus the HEN and MEN interact with each other. One can now concentrate on the MEN alone analyzing how changes in stream flow rates, compositions and

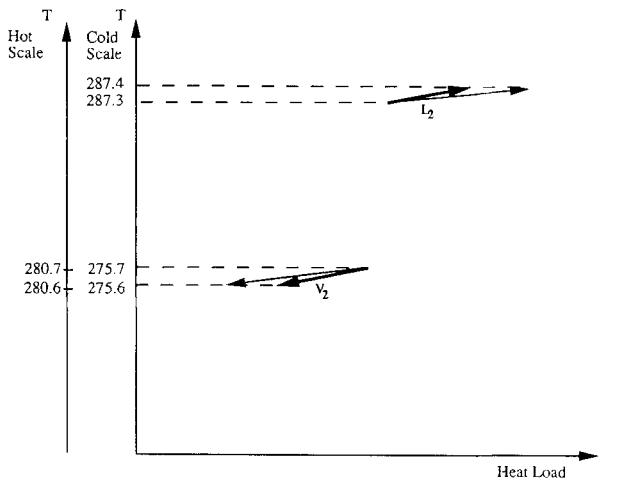

Figure 26. Effect of changes of reflux ratio on the HEN pinch diagram.

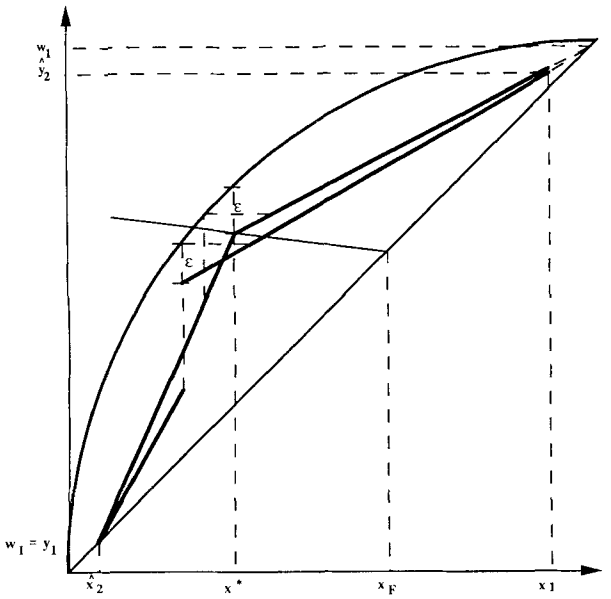

Figure 27. Effect of feed plate location on the McCabe-Thiele diagram.

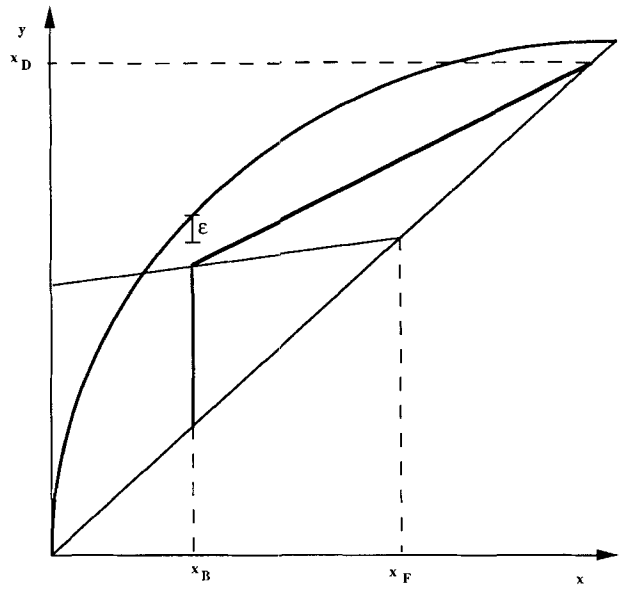

Figure 29. McCabe-Thiele diagram for an unpinched design.

enthalpies, which take place at the level of the distribution network, can reduce the flow rates of the streams that go to the MEN without altering their specific HEN inlet- and outlet-specific enthalpies.

Since no external mass-separating agents are employed, the mass load of the composite-rich and lean streams are equal. Moreover, since the pairs of streams V_1, L_2 and V_2, L_1 exchange mass in two different mass exchangers, the mass loads of V_1 and V_2 are equal to the mass loads of L_2 and L_1, respectively. This, in turn, means that inlet concentrations of V_2 and L_2, which are pinch candidate concentrations, share the same abscissa.

As the reflux ratio R is reduced, flow rates V_1, V_2, L_1, and L_2 are also reduced. In turn, the mass loads will also be reduced,

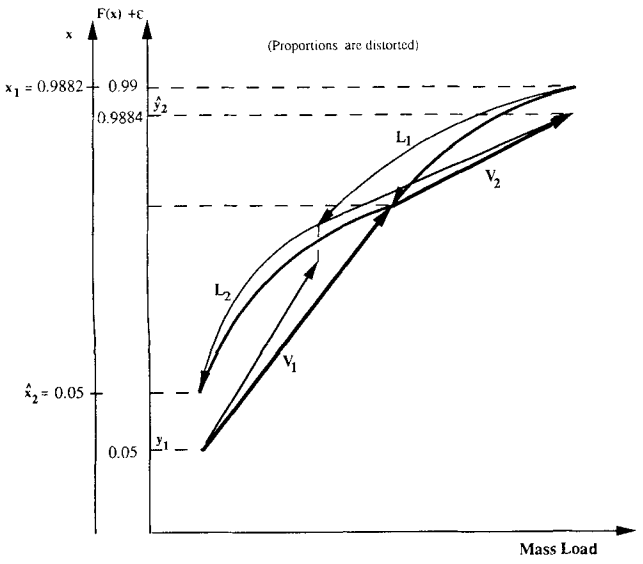

Figure 28. Effect of feed plate location on the MEN pinch diagram.

since the concentration at the end of the rich composite stream are fixed. The changes in the HEN and the MEN are shown in Figures 25–26. As slopes increase, the distance between the end points of streams V_1 and L_1 is reduced, and eventually the two composite streams touch, thus determining a pinch point. A further decrease in R will result in a crossing of the composite streams, revealing an infeasibility for that particular value of ϵ.

Pinch points of the MEN can be easily identified in the McCabe-Thiele operating line diagram. They correspond to concentrations of vapor and liquid, where the operating lines and the equilibrium curve are at a distance equal to the minimum approach ϵ.

The composite-rich and -lean streams are continuous (discontinuous) if the position of the feed plates straddles (does not straddle) the intersection of the operating lines in the y-x diagram. This can be easily established through material and energy balances at the feed plate and is illustrated in Figures 27 and 28. As this discontinuity is introduced and since the end concentration levels of the lean composite stream remain unaltered, a reduction of slopes must take place to maintain the operating lines at a distance ϵ from the equilibrium curve. Since the rich composite stream must have the same load, rich-stream slopes must also decrease. The effect is expressed in the HEN through a reduction of slopes and an increase in the utility load. This discontinuity also manifests itself in the McCabe-Thiele diagram. Indeed, as the intersection point of the operating lines is not straddled, the upper operating line has its end point at a liquid concentration which is lower than the abscissa of the intersection point. As $\hat{x}_1 = x_2$, the lower operating line ends at the same abscissa, but at a lower ordinate. If the feed stream is a two-phase stream, discontinuities of both composite streams in the C-ML diagram will be observed, whereas a single discontinuity will be observed in the rich composite stream for a subcooled liquid feed stream. In all three cases, these discontinuities must be avoided if minimum utility consumption is sought.

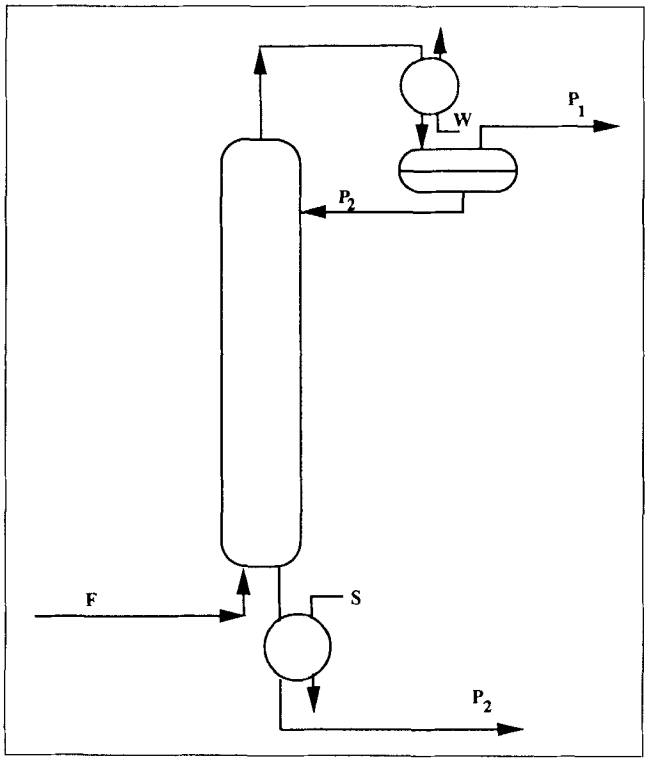

Figure 30. Unpinched distillation column.

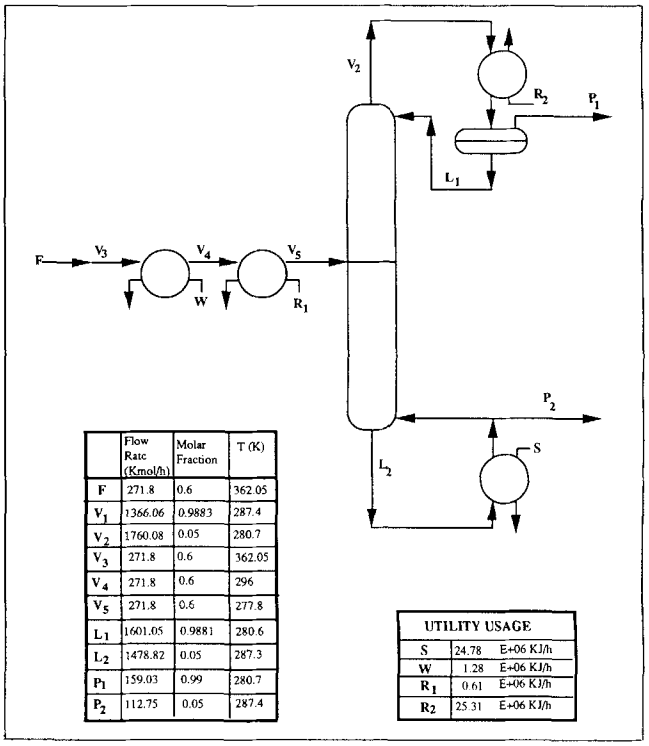

	Flow Rate (Kmol/h)	Molar Fraction	T (K)
F	271.8	0.6	362.05
V_1	1366.06	0.9883	287.4
V_2	1760.08	0.05	280.7
V_3	271.8	0.6	362.05
V_4	271.8	0.6	296
V_5	271.8	0.6	277.8
L_1	1601.05	0.9881	280.6
L_2	1478.82	0.05	287.3
P_1	159.03	0.99	280.7
P_2	112.75	0.05	287.4

UTILITY USAGE		
S	24.78	E+06 KJ/h
W	1.28	E+06 KJ/h
R_1	0.61	E+06 KJ/h
R_2	25.31	E+06 KJ/h

Figure 31. One-column design for the C3 problem with precooling.

Finally, let us consider the case of the McCabe-Thiele diagram of Figure 29. If minimum utility is sought, then the lower operating line should have infinite slope (negative slopes of this line do not have physical meaning, since they represent negative flow rates). The feed plate for such design is at the bottom (Figure 30). If the intersection of the operating lines is at a distance from the equilibrium curve which is greater than ϵ, there is no pinch point possible. It is easy to see that the corresponding MEN has only one rich and one lean stream.

Effect of heat integration

Let us now consider other alternative designs, which involve precooling of the feed stream either through external coolants (Figure 31) or through heat integration with existing cold streams or any combination thereof (Figure 32). Both designs are considered by the state-space realization shown in Figure 33.

To analyze the beneficial effect of heat integration, a common basis of comparison should be established. One such common basis is achieved when for every amount of precooling, the resulting distillation column is designed to minimize its utility consumption: that is, internal flow rates are such that a pinch point at the end of L_1 is established. To identify each level of precooling one can use the value of the parameter q of the column's feed stream. Figure 34 shows the changes seen in the MEN as the value of q corresponding to the mixture fed to the column varies. The net effect of increasing the precooling is to move the pinch point to higher values, increasing L_2 and decreasing V_2. The corresponding effect on the HEN is shown in Figure 35, where heat integration has been considered. As q increases, the temperature of the column's feed stream decreases. This decrease increments the amount of heat that can be integrated by establishing the only feasible match (V_3 with L_2). Therefore, the amount of heat ($Q^{VL}_{3,2}$) that the feed stream V_3 can release to the reboiler stream

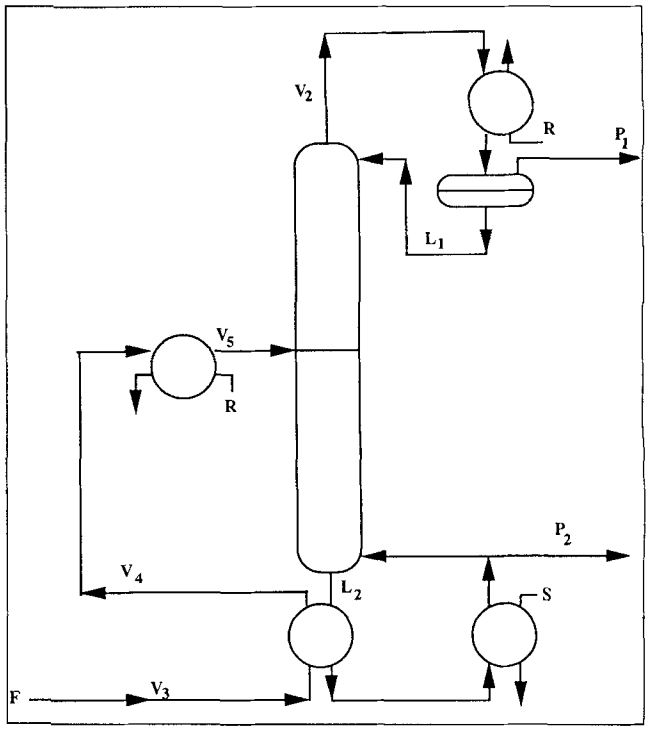

Figure 32. One-column design for the C3 problem with precooling and heat integration.

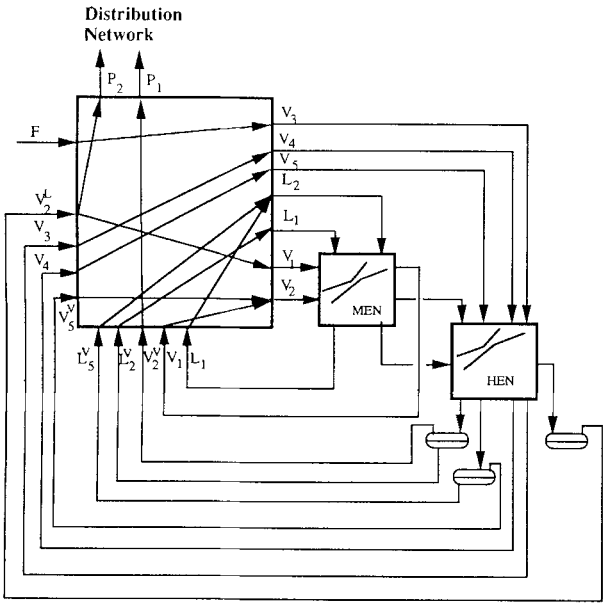

Figure 33. State-space realization of a single-column design for the C3 problem (with precooling).

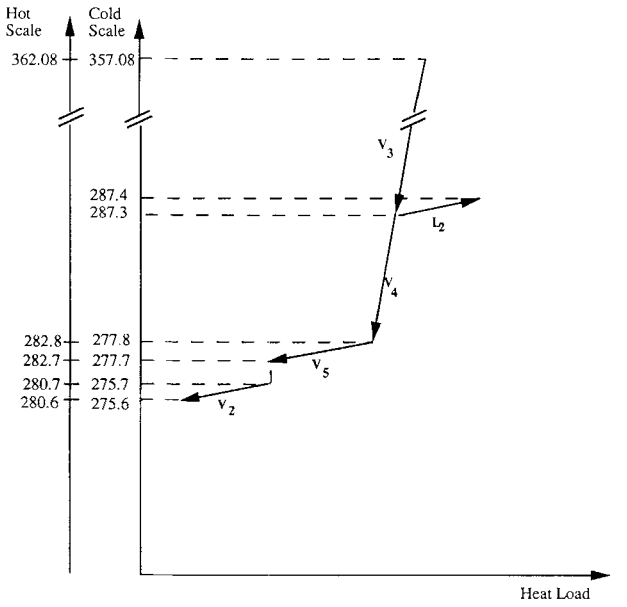

Figure 35. Effect of precooling in the HEN pinch diagram.

L_2 increases. As precooling continues to increase, the temperature difference between the exit temperature of the feed stream $\tilde{T}_3^V$ and the temperature of L_2 (T_2^L) decreases eventually reaching the minimum approach ΔT. At this point, the amount of heat $Q_{3,2}^{VL}$ has reached its maximum value. Further increase of precooling requires the use of refrigerant, and therefore $Q_{3,2}^{VL}$ stays at its maximum value. Therefore, if heat integration is chosen to take place, the refrigerant usage to achieve the desired level of precooling (desired q for the column's feed stream), remains zero until q reaches the value corresponding to feasible maximum heat exchange and increases from then on.

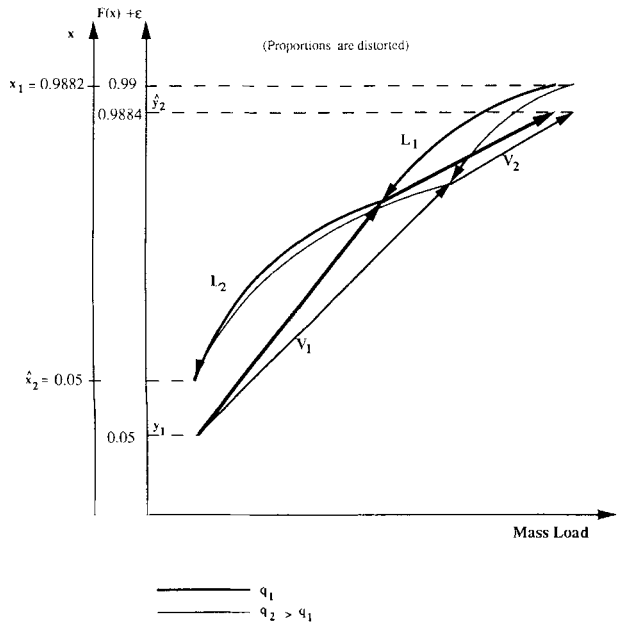

Figure 34. Effect of precooling in the MEN pinch diagram.

On the other hand, as q increases, the internal flow rates of the column decrease, and so does the utility load of the condenser. For this reason, the combined overall cold utility usage passes through a minimum.

For the same reason, the hot utility cost passes through a minimum, when heat integration is present and monotonically increases if heat integration is not allowed. The presence of the minima for the hot utility is related to the value of the maximum amount of heat that can be exchanged. If this value is small, the minimum may not even appear.

The combined effect to give the overall utility cost depends on the relative cost of the two utilities. For example, if the cold utility is cheaper than the hot utility as in the case of cooling water and steam, the optimum may be located near the minimum of the hot utility cost. Likewise, if the cold utility is more expensive, as it happens when using steam and refrigerant in low-temperature distillation such as in the C3 splitting, the optimum will be located near the optimum of the cold utility.

Other state-space designs

From the above analysis, it is clear that the goal of any improvement from these basic designs has to be based on the reduction of reboiler and/or condenser loads combined with a maximization of heat integration, whenever possible. This has already been done to the maximum extent for the designs outlined above.

The state-space model provides other alternatives that can be explored.

Consider the best design obtained (Figure 32) as a starting basis. The state-space realization of this design has been shown in Figure 33. Many of the available connections in the DN were not used. We turn our attention to those DN internal flow rates that are not considered by the previous designs. In particular, we are interested in determining if nonzero flow

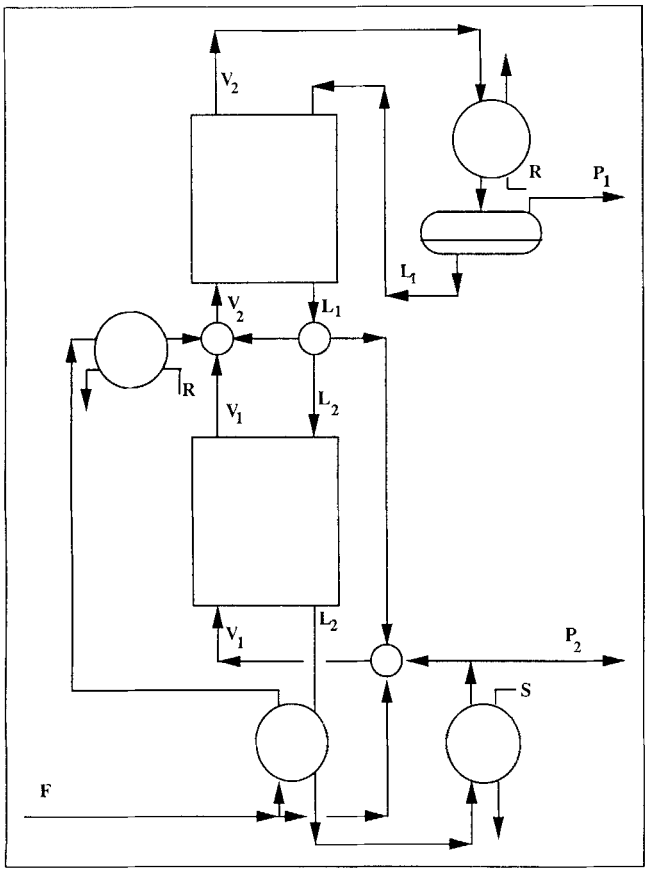

Figure 36. Liquid-bypassed state-space design of a single column with superheated feed.

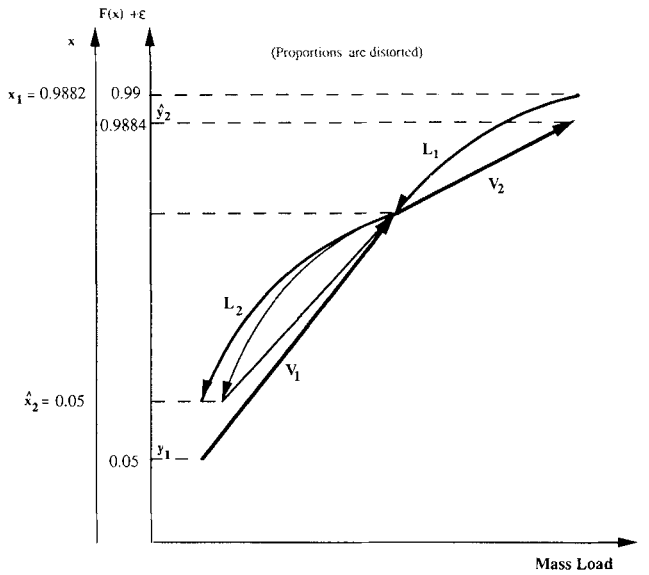

Figure 37. Effect of liquid bypassing on the MEN pinch diagram.

rates of any of these connections can help in reducing flow rates V_2 and L_2. We concentrate on L_2 first.

Since total and component mass balances must be satisfied, the only possibility of reducing L_2 is by activating a connection inside the DN that constitutes some bypass, which will not alter other flow rates. One of these bypasses is established by activating $L^{LV}_{1,1}$, as shown in Figure 36. To keep material balances satisfied, $L^{LL}_{1,2}$ is reduced by the same amount. Although the total material balance is satisfied, several other effects take place. First, the reduction in flow rate, experimented by L_2, results in a change of slope of L_2 in the C-ML diagram. Second, the effect of the bypassing also raises the concentration of V_1. Finally, V_1 becomes a two-phase stream. This last effect needs to be compensated, either by heating the bypassing stream to the appropriate energy level or by introducing an additional superheated stream that would adjust the enthalpy by mixing. (A saturated stream cannot be used, since the resulting mixture would never be a saturated vapor.) As all possibilities of heat integration are already exhausted, heating of the bypass will result in an overall hot utility consumption similar to the design obtained in Figure 32, whereas use of part of the only superheated stream available, F_1, is beneficial in two ways. On the one hand, heating utility usage is avoided, and on the other, precooling using refrigerant after heat integration is reduced.

The greater the enthalpy of the "heating stream," the greater the amount of bypass $L^{LV}_{1,1}$ can be used. Since V_3 and F_1 have the same concentration having greater enthalpy, the usage of F_1 is preferred over V_3. The improved design will be called the "liquid-bypassed" design (Figure 36).

The effect on the MEN pinch diagram in Figure 37 is to increase the slope of L_2 and decrease the slope of V_1, while maintaining $\hat{x}_2$ fixed and increasing y_1. The amount of mass exchanged is lower too. The effect on the McCabe-Thiele diagram is shown in Figure 38.

The value of y_1, however, cannot increase beyond its limit $y^* = F(\hat{x}_2) - \epsilon$ at which a second pinch point is obtained.

Other bypasses are less beneficial. For example, a bypass of the liquid stream going to the reboiler starting at a lower composition (see Figure 39) has the effect of reducing the

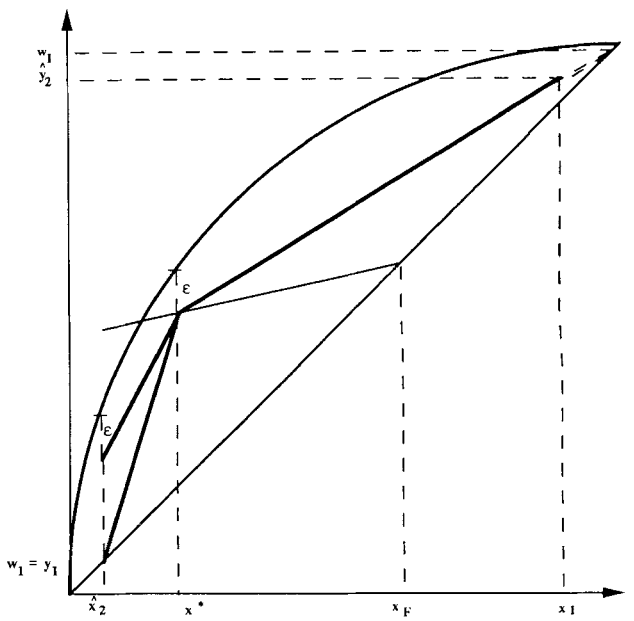

Figure 38. Effect of liquid bypassing on the McCabe-Thiele diagram.

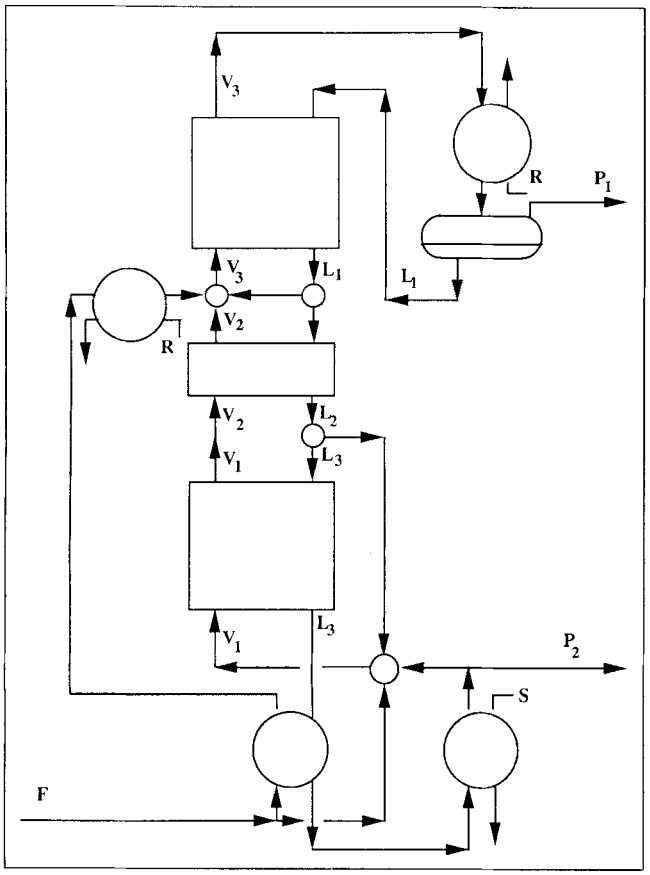

Figure 39. Liquid bypassed state-space design of a single column with superheated feed.

Bypassing at low concentrations.

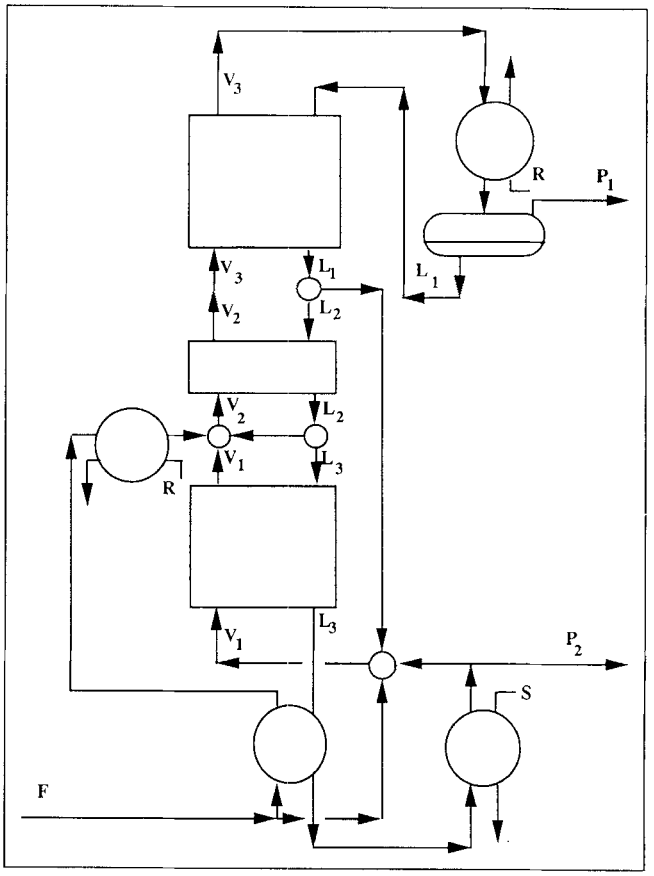

Figure 40. Liquid bypassed state-space design of a single column with superheated feed.

Bypassing at high concentrations.

amount of heating stream $F^V_{1,1}$ required to obtain a saturated vapor stream V_1.

Bypassing part of L_1 and L_2, as shown in Figure 40, cannot be performed without altering the vapor inlet composition y_2 of the upper mass exchanger. As the liquid flow rate is smaller, while the vapor flow rate remains the same, a component balance in the upper mass exchanger dictates an increase in y_2. This, in turn, suggests that the minimum approach already obtained in the lower end of the operating line corresponding to this exchanger will now be violated. The only way to compensate for this is to increase flow rates, which in turn results in an increase of utility usage. Therefore, these bypasses cannot improve the energy efficiency of a conventional distillation column.

In a similar way, one may try to reduce the flow rate of stream V_2 by introducing a bypass $V^{VL}_{1,1}$. Since L_1 needs to be saturated, a "cooling" stream is needed. This stream, which cannot be a saturated liquid, is present only if the feed is subcooled.

The above improving procedure may be performed using any other design of different q value as a starting basis.

There, however, is another alternative to reduce the energy consumption. Suppose that the bottom liquid concentration $\hat{x}_2$ is lowered and that stream L_2 is only partially heated in the reboiler producing a two-phase output stream. Later the liquid portion of this stream is mixed with the feed stream, whereas the vapor is fed to the column again. Such a design is shown in Figure 41 and will be called "feed-bypassed" design. Figures 42 and 43 show the changes in the MEN and McCabe-Thiele operating line diagrams, respectively. As a result of the reduction of the feed into the column, the liquid flow rate L_2 decreases, which leads to a decrease in hot utility. Partial reboiling also decreases the hot utility consumption.

The above exact same two solutions have also been found by employing the optimization package MINOS to optimize the interaction of MEN/HEN. The costs are compared in Table 4. Although the "feed-bypassed" and the "liquid-bypassed" designs are similar in cost for the C3 case study, this is not necessarily true in general.

The above discussion should not be interpreted as if all possibilities of improvement have been exhausted. If one allows more streams in the DN or different MEN at various pressure levels, richer configurations featuring lower utility consumption may be possible to obtain.

Distillation designs of the multi-effect type

Multi-effect distillation is a name coined for special multi-pressure distillation networks (King, 1980; Grant, 1979). They consist of two (or more) columns functioning at different pressures. As pressure changes, so do the dew and bubble points of the mixture; at some point the heat released by the condenser

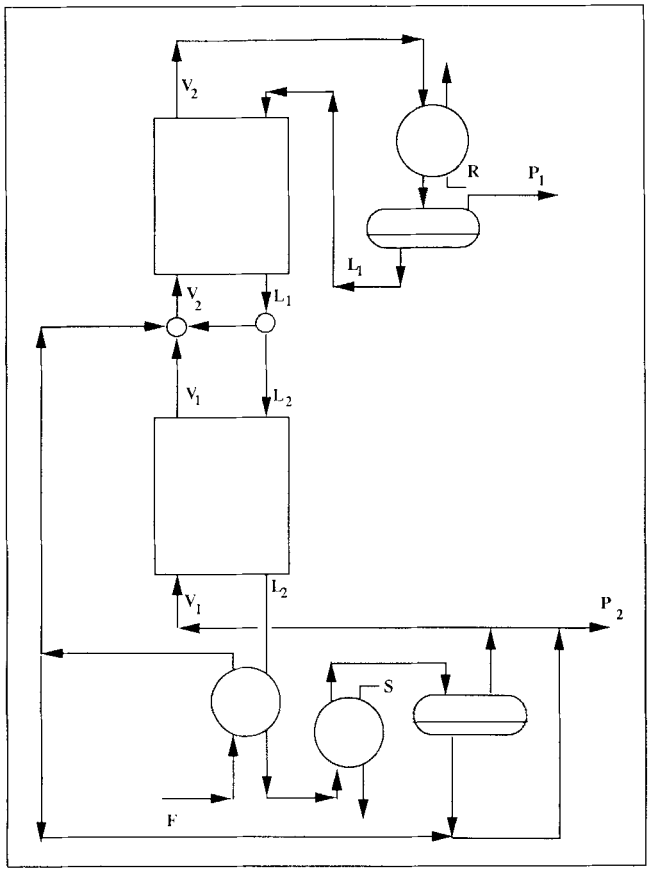

Figure 41. Feed bypassed state-space design of a single column with superheated feed.

of a high-pressure column can be used in the reboiler of a low-pressure column. The convenience of these designs and their placement into overall process design were discussed by Linnhoff et al. (1983) and Smith and Linnhoff (1988). Andrecovich and Westerberg (1985) showed how to calculate utility bounds

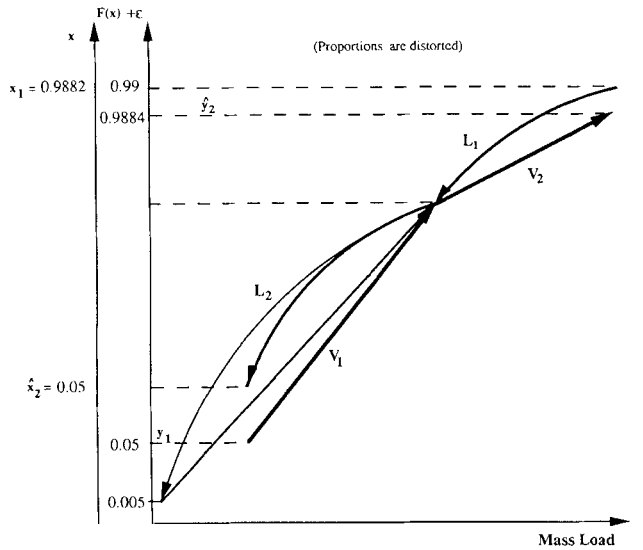

Figure 42. Effect of feed bypassing on the MEN pinch diagram.

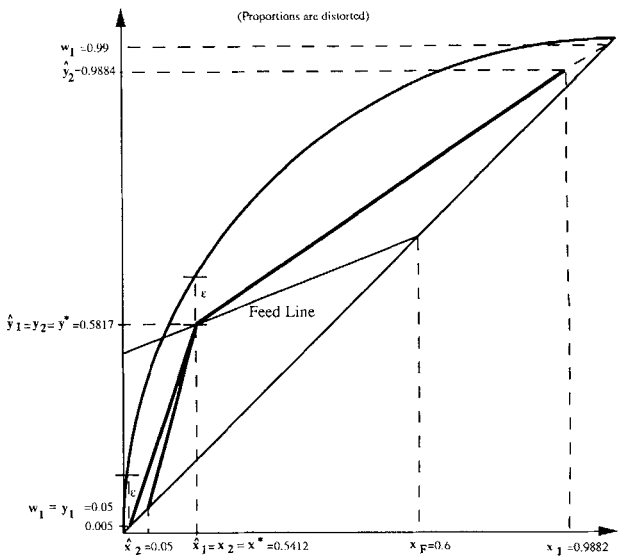

Figure 43. Effect of feed bypassing on the McCabe-Thiele diagram.

for the case in which one-feed, two-product distillation columns are used in a multi-effect context.

A traditional two-column multi-effect design is shown for the C3-splitting problem in Figure 44. Flow rates and properties of different streams are given in Table 5. A heat pump operating with propane between 70 psia (482 kPa) and 350 psia (2,412 kPa), has been included for this case. Both columns operate at a reflux ratio such that the utility usage in the condenser of the low-pressure column (refrigerant) and the reboiler of the high-pressure column (steam) are minimized; that is, the intersection of operating lines is at a distance ϵ from the equilibrium curve. Any other splitting ratio requires that one of the columns operates with a higher reflux ratio and therefore consumes more utility.

As was done for the case of one-column, one can start introducing all the changes suggested by the state-space model. That is, one may introduce "liquid-bypassed" designs or "feed-bypassed" designs for both columns. The resulting HEN/MEN interactions will eventually result in a reduced utility cost.

The possibilities suggested by the state-space model, however, are not confined to the aforementioned individual column improvements. Moreover, as now the reboiler of the low-pressure column is heat-integrated with the condenser of the high-pressure stream, there is no direct utility cost associated with it. Therefore, the incentive to reduce its load may be found in its effect in the load of other streams, such as the condenser of the same column. As it is not possible to be sure that one has explored all evolutionary steps suggested by the state-space approach, an optimization procedure was used. Split-matching

Table 4. One-Column Costs for the C3 Problem (without Heat Pump)

	($/h)
Direct Feed	120.5
With Heat Integration (Fig. 25)	116.7
Liquid-Bypassed	115.2
Feed-Bypassed	115.2

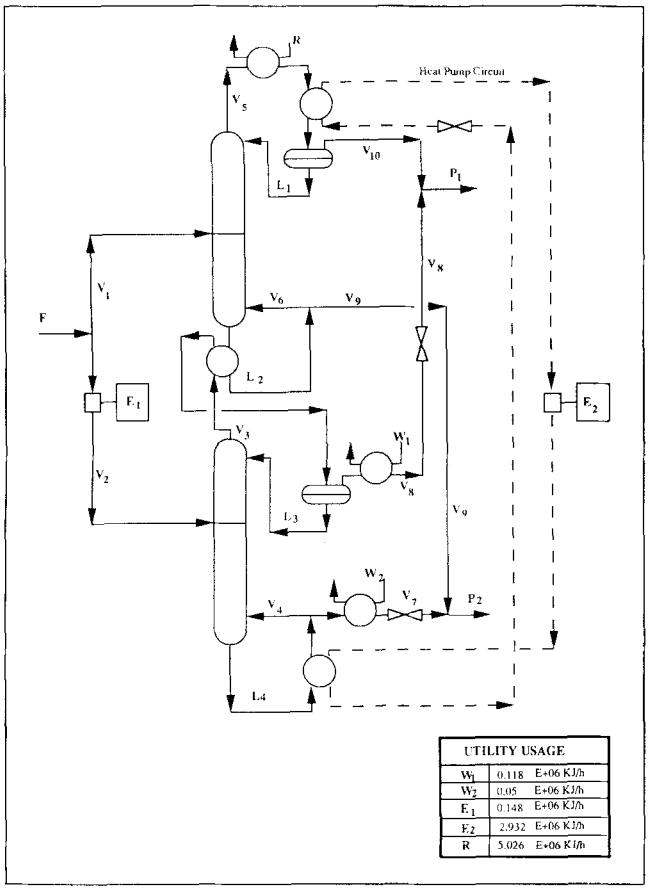

Figure 44. Two-column multi-effect flowsheet for the C3 problem.

operators were included in the model, and MINOS was used to obtain the results. One network realizing the results obtained using a heat pump is shown in Figure 45. Flow rates and properties of different streams are given in Table 6.

Table 5. Conventional Multi-Effect Solution of the C3 Problem (Figure 44)

Stream	Flow Rate (Kmol/h)	Molar Fraction	Pres. (psia)	T (K)
F	271.8	0.6	106	362.05
V1	147.69	0.6	106	362.05
V2	124.09	0.6	300	397.03
V3	1,131.71	0.9888	300	322.08
V4	935.21	0.05	300	331.2
V5	956.39	0.9883	106	280.7
V6	742.29	0.05	106	287.4
V7	51.49	0.05	300	330.0
V8	72.61	0.99	300	321.7
V9	61.27	0.05	106	287.4
V10	86.41	0.99	106	280.6
L1	869.98	0.9881	106	280.6
L2	803.56	0.05	106	287.4
L3	1,059.09	0.9887	300	322.8
L4	986.70	0.05	300	331.2
P1	159.03	0.99	106	280.7
P2	112.75	0.05	106	287.4

SI conversion: kPa = psi × 6.89

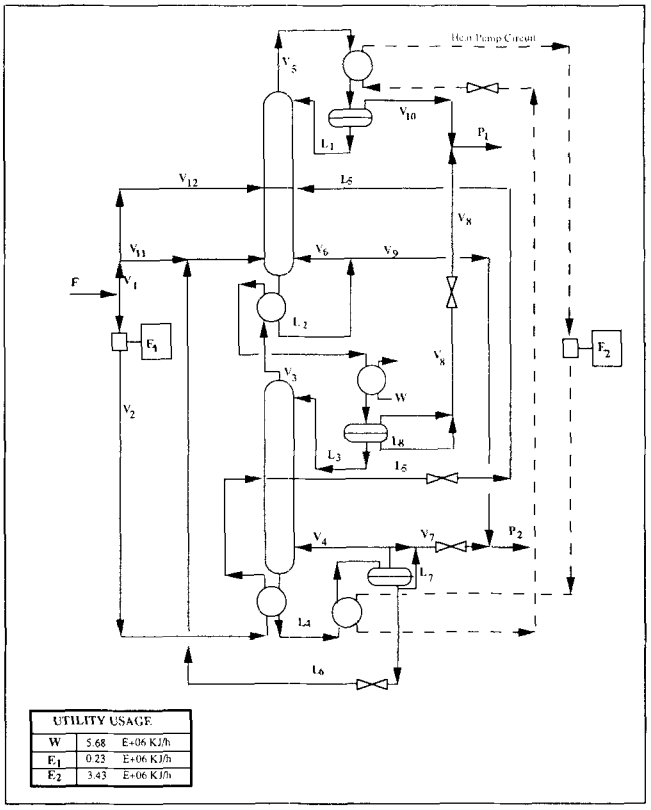

Figure 45. Two-column state-space flowsheet for the C3 problem.

The high-pressure column is a combination of a "feed-bypassed" and a "liquid-bypassed" column. Instead of bypassing streams, the low-pressure column receives a contribution of liquid from the high-pressure liquid drum, which, together

Table 6. State-Space Multi-Effect Solution of the C3 Problem (Figure 45)

Stream	Flow Rate (Kmol/h)	Molar Fraction	Pres. (psia)	T (K)
F	271.8	0.6	106	362.05
V1	78.5	0.6	106	362.05
V2	193.3	0.6	300	397.03
V3	1,413.9	0.99044	300	322.1
V4	1,204.0	0.00817	300	331.2
V5	724	0.98625	106	280.7
V6	593.3	0.08156	106	287.1
V7	48.5	0.00758	300	331.2
V8	92.5	0.9913	300	321.7
V9	64.4	0.08156	106	287.1
V10	66.4	0.98819	106	280.6
V11	65.9	0.6	106	362.05
V12	12.6	0.6	106	362.05
L1	657.68	0.98605	106	280.6
L2	803.56	0.08156	106	287.0
L3	1,321.3	0.99038	300	322.8
L4	1,263.1	0.00816	300	331.1
L5	41.5	0.57003	300	305.6
L6	10.7	0.00727	300	331.1
L7	3.8	0.00816	300	331.1
L8	12.3	0.99038	300	331.1
P1	159.03	0.99	106	280.7
P2	112.75	0.05	106	287.4

Table 7. Multi-Effect-Type Costs of the C3 Problem

	($/h)
Conventional	51.2
State Space	46.8

with a small contribution of the low-pressure feed stream, results in an increase of the concentration of the bottom inlet vapor. Also, part of the liquid extracted from the middle of the high-pressure column is used to reduce the superheating state of the low-pressure feed. Costs are compared in Table 7.

Multifeed distillation networks

To further illustrate the concept of state space as applied to distillation networks we investigate a two-feed, two-product problem. This case study represents a typical separation problem in the microelectronics industry. Consider a solvent used for cleaning purposes and water used to rinse the remaining portions of solvent from the cleaned material. As a result of this process, the solvent stream is contaminated with water, and the water stream is contaminated with solvent. It is desired to design a distillation network that would perform the regeneration of both streams to their desired purity for reuse. The feed and desired product stream data are given in Table 8. Costs of steam and cooling water are the same as those given in Table 3. A heat pump is not included.

Some designs can be suggested to perform this separation. For example, separating each stream in one column is more expensive than a one-column, two-feed design shown in Figure 46. In this design, the solvent-rich-stream feed plate coincides with the bottom column plate, and the design is unpinched.

The state-space solution obtained using the optimization model departs significantly from the previously presented designs. Figure 47 shows one network that realizes the solution

Table 8. Data for the Multifeed Solvent Separation Problem

Feeds:			
180.84	kmol/h	$z1 = 0.99$	@Sat. Vapor
107.41	kmol/h	$z2 = 0.01$	@Sat. Vapor
Products:			
179.811	kmol/h	$z1 = 0.999999$	@Sat. Liquid
108.447	kmol/h	$z1 = 0.002746$	@Sat. Vapor
Thermodynamic Data:			
Pressure:		0.1 atm	
Solvent Boiling Point:		410. 4 K	
Water Boiling Point:		327. 4 K	
Relative Volatility:		64.475	
Enthalpy coefficients:			
Liquid:		$a =$ 25,660 kJ/kmol	
		$b = -21{,}570$ kJ/kmol	
Vapor:		$a =$ 79,570 kJ/kmol	
		$b = -32{,}700$ kJ/kmol	
Temperature Coefficients:			
Dew Point:		$d1 =$ 410.87	
		$d2 = -166.88$	
		$d3 =$ 404.09	
		$d4 = -320.67$	
Bubble Point:		$c1 =$ 410.87	
		$c2 = -326.11$	
		$c3 =$ 436.76	
		$c4 = -194.12$	

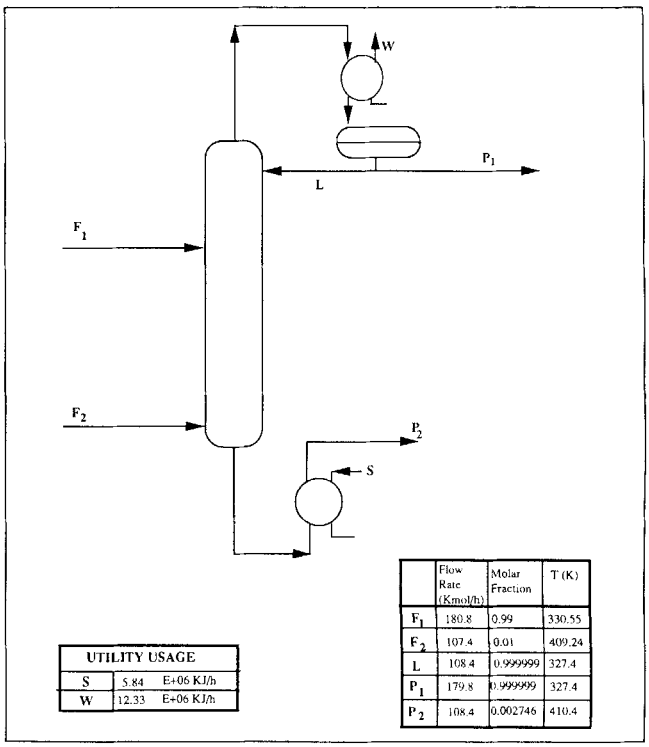

Figure 46. Multifeed solvent separation column.

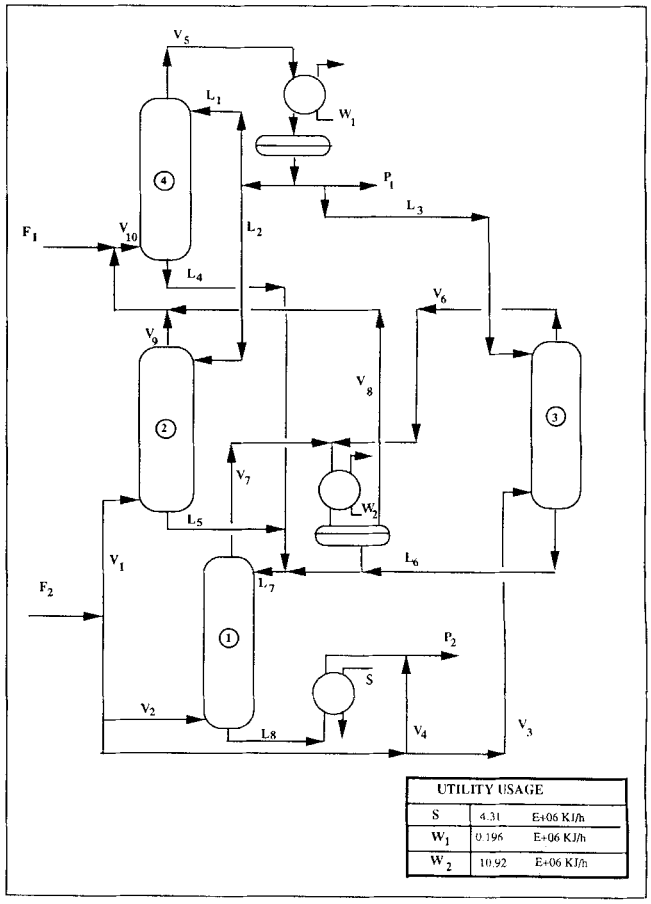

Figure 47. State-space solution for the multifeed distillation problem.

Table 9. State-Space Multifeed Solvent Separation Problem (Figure 47)

Stream	Flow Rate (Kmol/h)	Molar Fraction	T (K)
F1	180.8	0.99	330.5
F2	107.4	0.01	409.2
V1	15.77	0.01	409.2
V2	55.82	0.01	409.2
V3	7.3	0.01	409.2
V4	28.53	0.01	409.2
V5	255.27	0.999999	327.4
V6	7.3	0.99062	330.4
V7	55.82	0.99062	330.4
V8	58.66	0.99810	330.4
V9	15.77	0.999999	327.4
V10	255.27	0.99248	330.5
L1	5.85	0.999999	327.4
L2	47.6	0.999999	327.4
L3	22.01	0.999999	327.4
L4	5.85	0.67197	330.1
L5	47.6	0.67197	330.1
L6	22.02	0.67197	330.1
L7	79.92	0.684	327.4
L8	79.92	0.000157	327.4
P1	179.8	0.999999	327.4
P2	108.4	0.002746	410.4

obtained. Table 9 shows the flow rates and properties of different streams. A bypass from the solvent-rich feed to the solvent-rich product is present, as in the one-column, feed-bypassed designs. Four columns are used in a pattern of mixing and splitting that does not resemble any known design. Essentially, the water-rich stream coming from the condenser is split into three streams. One is used to enrich the water-rich feed stream (column 4). The other two are used to enrich in water part of the solvent-rich streams in two different columns (columns 2 and 3). After exchanging water, these three liquid streams mix and exchange again water with the remaining part of the solvent-rich stream, ending up with a concentration which is lower than the specified solvent-rich product (column 1). This liquid stream is sent to the reboiler and mixes with

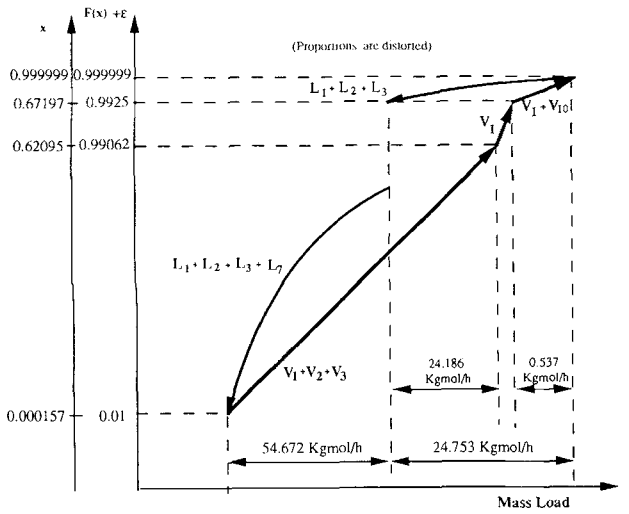

Figure 48. MEN pinch diagram for the multifeed solvent separation problem.

Table 10. Multifeed Solvent Separation Costs

	($/h)
One-Column (Two-Feed)	134.05
State Space	104.04

part of the solvent-rich stream. A vapor stream coming from the partial condenser of stripping column 4 mixes with the water-rich feed stream, whereas the liquid is sent as a reflux to the column. The corresponding MEN pinch diagram is shown in Figure 48. Pinch points are observed at the lower and upper ends of the composite streams. The corresponding HEN pinch diagram consists of three streams, one cold and two hot; as there is no heat integration, steam and cooling water are used.

Costs of different configurations are compared in Table 10. Basically, the large utility cost improvement is due to the "feed-bypass" pattern associated with the solvent-rich stream. As there is no need to heat this bypass, the cost savings in the reboiler are of the order of 26.6%. The cooling duty of the two condensers in the state-space solution, however, is higher than the condenser duty of the one-column, two-feed configuration. The net overall utility cost savings are 22.4%.

Conclusions

The state-space apprcach to process synthesis has been applied to the problem of determining energy-efficient distillation networks. Results show that this approach can provide distillation network designs that are more energy-efficient than conventional ones.

The results also suggest that distillation, although a mature technology, needs to be re-examined at its fundamental level and be studied as a composite heat- and mass-exchange network.

Acknowledgment

Financial support from the UCLA-NSF-ERC under grant no. CDR 86-22184 and The Parsons Foundation under grant no. L900926 are gratefully acknowledged. We thank Ashish Gupta for his help in performing some of the computations.

Notation

a = enthalpy function parameter
A = linear operator of a single-input single-output time-invariant system; area of heat exchanger
b = enthalpy function parameter
B = linear operator of a single-input single-output time-invariant system
cp = heat capacity of streams
c = coefficient for bubble point calculations
C = flow rate of cold streams in the pinch operator; linear operator of a single-input single-output time-invariant system
$\tilde{H}$ = enthalpy of a stream at the outlet of the HEN or a separator
d = coefficient for dew point calculations
D = linear operator of a single-input single-output time-invariant system
E = electricity consumption (energy units)
F = flow rate of a feed stream
$F(x)$ = equilibrium composition of a vapor phase in contact with a liquid phase of composition x
G = flow rate of hot streams in the pinch operator
$G(y)$ = inverse of $F(x)$

H = enthalpy of a stream at the inlet of the HEN or a separator
L = liquid stream flow rate
p = auxiliary compositions in the pinch operator
$\hat{p}$ = auxiliary compositions in the pinch operator
P = flow rate of a product stream
q = parameter in the McCabe-Thiele method characterizing the phase state of the feed
Q = heat or mass released or gained by a stream in the pinch operator; heat or mass exchanged in the split-matching operator
R = refrigerant utility consumption (energy units); reflux ratio; auxiliary temperature in the HEN pinch operator
$\tilde{R}$ = auxiliary temperature in the HEN pinch operator
r = auxiliary compositions in the pinch operator
$\hat{r}$ = auxiliary compositions in the pinch operator
s = auxiliary compositions in the pinch operator
$\hat{s}$ = auxiliary compositions in the pinch operator
S = steam utility consumption (energy units)
t = auxiliary compositions in the pinch operator
$\hat{t}$ = auxiliary compositions in the pinch operator
T = temperature of a stream at the inlet of HEN
$\tilde{T}$ = temperature of a stream at the outlet of HEN
$u^{(j)}(t)$ = scalar valued input time function of a single-input, single-output time-invariant system
U = auxiliary temperature in HEN pinch operator
$\tilde{U}$ = auxiliary temperature in HEN pinch operator
v = temperature/composition of a stream at the inlet of a split-matching operator
$\tilde{v}$ = temperature/composition of a stream at the inlet of a split-matching operator
V = vapor stream flow rate
w = composition of a product stream
w_0^j = initial condition of a single-input, single-output, time-invariant system
$w^{(i)}(t)$ = scalar valued output time function of a single-input, single-output, time-invariant system
W = cooling water utility consumption (energy units)
x = liquid stream composition at the outlet of DN
$\hat{x}$ = liquid stream composition at the outlet of MEN
$\tilde{x}$ = liquid stream composition at the outlet of a separator
y = vapor stream composition at the outlet of DN
$\hat{y}$ = vapor stream composition at the outlet of MEN
$\tilde{y}$ = vapor stream composition at the outlet of a separator
$z(t)$ = state vector of a single-input, single-output, time-invariant system
z_0 = initial state vector of a single-input, single-output, time-invariant system
z = composition of a feed stream
$Z(T)$ = enthalpy function for the pinch operator

Greek letters

ϵ = minimum approach in MEN pinch and split-matching operators
ΔT = minimum approach in HEN pinch and split-matching operators
$\Delta T\ln$ = logarithmic mean temperature difference in a heat exchanger
Λ = large number
η = integer variable
ω = change in enthalpy due to compression

Supraindices

h = heat exchanged (split-matching operator)
m = mass exchanged (split-matching operator)
L = liquid stream flow rate
LL = connection between a liquid and a liquid junction in DN; liquid-state parameter for separators of cold liquid streams
LP = connection between a liquid and a product junction in DN
LV = connection between a liquid and a vapor junction in DN; vapor-state parameter for separators of cold liquid streams
V = vapor stream flow rate
VL = connection between a vapor and a liquid junction in DN; liquid-state parameter for separators of hot water streams
VP = connection between a vapor and a product junction in DN
VV = connection between a vapor and a vapor junction in DN; vapor-state parameter for separators of hot water streams

Subindices

bub = bubble point
dew = dew point

Literature Cited

Andrecovich, M. J., "Synthesis of Heat-Integrated Distillation Sequences," PhD Diss., Carnegie-Mellon Univ., Pittsburgh, PA (1983).

Andrecovich, M. J., and A. W. Westerberg, "A Simple Synthesis Method Based on Utility Bounding for Heat Integrated Distillation Sequences," *AIChE J.*, **31**, 363 (1985).

Bagajewicz, M. J., and V. Manousiouthakis, "On the Generalized Benders Decomposition," *Comp. & Chem. Eng.*, **15**(10), 691 (1991).

Bjorn, I., U. Gren, and K. Strom, "A Study of a Heat Pump Distillation Column System," *Chem. Eng. Process.*, **29**, 185 (1991).

Carlberg, N. A., and A. W. Westerberg, "Temperature-Heat Diagrams for Complex Columns: 2. Underwood's Method for Side Strippers and Enrichers," *Ind. Eng. Chem. Res.*, **28**, 1379 (1989).

Carlberg, N. A., and A. W. Westerberg, "Temperature-Heat Diagrams for Complex Columns: 3. Underwood's Method for the Petlyuk Configuration," *Ind. Eng. Chem. Res.*, **28**, 1386 (1989).

Cerda, J., A. W. Westerberg, D. Mason, and B. Linnhoff, "Minimum Utility Usage in Heat Exchanger Network Synthesis—A Transportation Problem," *Chem. Eng. Sci.*, **38**, 373 (1983).

Dundorf, J. A., and B. Linnhoff, "Energy Savings by Appropriate Integration of Distillation Columns into Overall Processes," ChE *Symp.*, Leeds, England (1982).

Duran, M. A., and I. E. Grossmann, "A Mixed-Integer Nonlinear Programming Approach for Process Systems Synthesis," *AIChE J.*, **32**(4), 592 (1986).

El-Halwagi, M. M., and V. Manousiouthakis, "Synthesis of Mass Exchange Networks," *AIChE J.*, **35**(8), 1233 (1989).

El-Halwagi, M. M., and V. Manousiouthakis, "Design and Analysis of Mass Exchange Networks with Multicomponent Targets," AIChE Meeting, paper 137f, San Francisco (1989).

El-Halwagi, M. M., and V. Manousiouthakis, "Simultaneous Synthesis of Mass-Exchange and Regeneration Networks," *AIChE J.*, **36**(8), 1209 (1990).

El-Halwagi, M. M., and V. Manousiouthakis, "Automatic Synthesis of Mass-Exchanger Networks with Single Component Targets," *Chem. Eng. Sci.*, **45**(9), 2813 (1990).

Finelt, S., "Better C3 Distillation Pressure," *Hydro. Process.*, 95 (Feb., 1979).

Floudas, C. A., "Separation Synthesis of Multicomponent Feed Streams with Multicomponent Product Streams," *AIChE J.*, **33**(4), 540 (1987).

Floudas, C. A., A. Aggarwal, and A. R. Ciric, "Global Optimum Search for Nonconvex NLP and MINLP Problems," *Comp. & Chem. Eng.*, **13**(10) (1990).

Floudas, C. A., and S. M. Anastasiadis, "Synthesis of Distillation Sequences with Several Multicomponent Feed and Product Streams," *Chem. Eng. Sci.*, **43**(9), 2407 (1988).

Floudas, C. A., A. R. Ciric, and I. E. Grossmann, "Automatic Synthesis of Optimum Heat Exchanger Network Configurations," *AIChE J.*, **32**, 276 (1986).

Floudas, C. A., and A. R. Ciric, "Strategies for Overcoming Uncertainties in Heat Exchanger Network Synthesis," *Chem. Eng. Sci.*, **13**(10), 1133 (1989).

Floudas, C. A., and G. E. Paules IV, "A Mixed Integer Nonlinear Programming Formulation for the Synthesis of Heat-Integrated Distillation Sequences," *Comp. & Chem. Eng.*, **12**(6), 531 (1988).

Grant, C., "Energy Conservation in the Chemical and Process Industries," Instn. of Chem. Engrs., London (1979).

Grossmann, I. E., and W. H. Sargent, "Optimum Design of Heat Exchanger Networks," *Comp. & Chem. Eng.*, **2**, 1 (1978).

Grossmann, I. E., "Mixed-Integer Programming Approach for the

Synthesis of Integrated Process Flowsheets," *Comp. & Chem. Eng.*, **9**(5), 463 (1985).
Grimes, L. E., "The Synthesis and Evolution of Networks of Heat Exchangers that Feature the Minimum Number of Units," MSc Thesis, Carnegie Mellon Univ. (1980).
Gundersen, T., and L. Naess, "The Synthesis of Cost Optimal Heat Exchanger Networks. An Industrial Review of the State of the Art," *Comp. & Chem. Eng.*, **12**(6), 503 (1988).
Holland, C. D., *Fundamental of Multicomponent Distillation*, McGraw-Hill, New York (1981).
Kaibel, G., E. Blass, and J. Kohler, "Design of Distillative Separation with Due Consideration of Thermodynamic Aspects," *Chem.-Eng.-Tech.*, **61**(1), 16 (1989).
Kailath, T., *Linear Systems*, Prentice Hall, New York (1980).
King, C. J., *Separation Processes*, 2nd ed., McGraw-Hill, New York (1980).
Knight, J. R., and M. F. Doherty, "Optimal Design and Synthesis of Homogeneous Azeotropic Distillation Sequences," *Ind. Eng. Chem. Res.*, **28**, 564 (1989).
Linnhoff, B., H. Dundorf, and R. Smith, "Heat Integration of Distillation Columns into Overall Processes," *Chem. Eng. Sci.*, **38**(8), 1175 (1983).
Lynd, L. R., and H. E. Greitland, "Distillation with Intermediate Heat Pumps and Optimal Sidestream Return," *AIChE J.*, **32**, 1350 (1986).
Mallick, S. K., "Synthesis of Separation Processes with Nonsharp Separators," *Chem. Eng. Sci.*, **46**(10), 2729 (1991).
Maraki, M., and T. Hayakawa, "Synthesis of a Multicomponent Multiproduct Separation Process with Nonsharp Separators," *Chem. Eng. Sci.*, **43**(2), 259 (1988).
McCabe, W. L., J. C. Smith, and P. Harriot, *Unit Operations of Chemical Engineering*, 4th ed., McGraw Hill, New York (1985).
Morari, M., and D. C. Faith, "The Synthesis of Distillation Trains with Heat Integration," *AIChE J.*, **26**, 916 (1980).
Naka, Y., M. Terashita, and T. Takamatsu, "A Thermodynamic Approach to Multicomponent Distillation Systems," *AIChE J.*, **28**(5), 812 (1982).
Nath, R., and R. L. Motard, "Evolutionary Synthesis of Separation Processes," AIChE Meeting, Philadelphia (1978).
Nath, R., and R. L. Motard, "Evolutionary Synthesis of Separation Processes," *AIChE J.*, **27**(4), 578 (1981).
Nikolaides, I. P., and M. F. Malone, "Approximate Design of Multifeed/Side-Stream Distillation Systems," *Ind. Eng. Chem. Res.*, **26**, 1839 (1987).
Nishida, N., G. Stephanopoulos, and A. W. Westerberg, "A Review of Process Synthesis," *AIChE J.*, **27**(3), 321 (1981).
Null, H. R., "Heat Pumps in Distillation," *Chem. Eng. Prog.*, **72**(7), 58 (1976).
Papoulias, S. A., and I. E. Grossmann, "A Structural Approach in Process Synthesis: I. Utility Systems," *Comp. & Chem. Eng.*, **7**, 695 (1983).
Papoulias, S. A., and I. E. Grossmann, "A Structural Approach in Process Synthesis: I. Heat Recovery Systems," *Comp. & Chem. Eng.*, **7**, 707 (1983).
Papoulias, S. A., and I. E. Grossmann, "A Structural Approach in Process Synthesis: I. Total Processing Systems," *Comp. & Chem. Eng.*, **7**, 723 (1983).
Petlyuk, F. B., F. J. Flatonov, and D. M. Slavinskii, "Thermodynamically Optimal Method for Separating Multicomponent Mixtures," *Int. Chem. Eng.*, **5**, 555 (1965).
Quadri, G. P., "Use Heat Pump for P-P Splitter," *Hydroc. Process.*, **60**(1), 147 (1981).
Rathore, N. S., K. A. Van Wormer, and G. J. Powers, "Synthesis Strategies for Multicomponent Separation Systems with Energy Integration," *AIChE J.*, **20**, 491 (1974).
Rathore, N. S., K. A. Van Wormer, and G. J. Powers, "Synthesis of Distillation Systems with Energy Integration," *AIChE J.*, **20**, 940 (1974).
Rudd, D. F., and C. C. Watson, *Strategy of Process Engineering*, Wiley, New York (1968).
Sahinidis, N. V., and I. E. Grossmann, "Convergence Properties of the Generalized Benders Decomposition," *Comp. & Chem. Eng.*, **15**(7), 481 (1991).
Sargent, R. W., and K. Gaminibandara, "Optimum Design of Plate Distillation Column," *Optimization in Action*, L. C. W. Dixon, ed., Academic Press, New York (1976).
Smith, R., and B. Linnhoff, "The Design of Separators in the Context of Overall Processes," *Chem. Eng. Res. Des.*, **66**, 195 (1988).
Terranova, B. E., and A. W. Westerberg, "Temperature-Heat Diagrams for Complex Columns: 1. Intercooled/Interheated Distillation Columns," *Ind. Eng. Chem. Res.*, **28**, 1374 (1989).
Tyreus, B. D., and W. L. Luyben, "Two Towers Cheaper than One," *Hydroc. Process.*, **54**(7), 93 (1975).
Umeda, T., N. Nishida, and K. Shiroko, "A Thermodynamic Approach to Heat Integration in Distillation," *AIChE J.*, **25**(3), 423 (1979).
Umeda, T., T. Harada, and K. Shiroko, "A Thermodynamic Approach to the Synthesis of Heat Integration Systems in Chemical Processes," *Comp & Chem. Eng.*, **3**, 273 (1979).
Wehe, R. R., and A. W. Westerberg, "An Algorithmic Procedure for the Synthesis of Distillation Sequences with Bypass," *Comp. & Chem. Eng.*, **11**(6), 619 (1987).
Wehe, R. R., and A. W. Westerberg, "A Bounding Procedure for the Minimum Number of Columns in Nonsharp Distillation Sequences," *Chem. Eng. Sci.*, **45**(1), 1 (1990).
Westerberg, A. W., "The Synthesis of Distillation-Based Separation Systems," *Comp. & Chem. Eng.*, **9**(5), 421 (1985).
Westerberg, A. W., "Synthesis in Engineering Design," *Comp. & Chem. Eng.*, **13**(3/4), 365 (1989).
Yee, T. F., I. E. Grossmann, and Z. Kravanja, "Simultaneous Optimization Models for Heat Integration: I. Area and Energy Targeting and Modeling of Multistream Exchangers," *Comp. & Chem. Eng.*, **14**(10), 1151 (1990).
Yee, T. F., and I. E. Grossmann, "Simultaneous Optimization Models for Heat Integration: II. Heat Exchanger Network Synthesis," *Comp. & Chem. Eng.*, **14**(10), 1165 (1990).
Zadeh, L. A., and C. A. Desoer, *Linear System Theory—The State Space Approach*, 2nd ed., Robert Krieger, New York (1979).

Appendix: The State Space Model

It is assumed that the problem has n_F feed streams and n_P product streams with concentrations z_n and w_r, and enthalpies H_n^F and H_r^P, respectively.

We create n_V vapor streams V_j, as well as n_L liquid streams L_i. Vapor streams have compositions y_j and enthalpy H_j^V, whereas liquid streams have composition and x_i and enthalpy H_i^L. After passing through the MEN, the molar flow rate of these streams remains the same (assumption e), whereas the composition and enthalpy changes to $\hat{y}_j$, $\hat{H}_j^V$ for vapor streams and to $\hat{x}_i$, $\hat{H}_i^L$ for liquid streams. After passing through the MEN, some streams go to the HEN and some go back to the DN.

Some streams do not go to the MEN, going directly to the HEN split-matching operator. All the compositions and enthalpies at the outlet of the HEN are $\tilde{y}_j$, $\tilde{H}_j^V$ for vapor streams and to $\tilde{x}_i$, $\tilde{H}_i^L$ for liquid streams. Finally, streams coming out of a phase separator corresponding to a liquid stream (L_i) have inlet and enthalpy concentration x_i (or $\hat{x}_i$) and $\tilde{H}_i^L$. The outlet liquid and vapor flow rates are L_i^L and V_i^L with concentrations $\tilde{x}_i^L$ and $\tilde{y}_i^L$ and enthalpies $\tilde{H}_i^{LL}$ and $\tilde{H}_i^{LV}$, respectively. Similarly, streams coming out of a phase separator corresponding to a vapor stream (V_j) have inlet and enthalpy concentration y_j (or $\hat{y}_j$) and $\tilde{H}_j^V$. The outlet liquid and vapor flow rates are L_j^V and V_j^V, respectively, with concentrations $\tilde{x}_j^V$ and $\tilde{y}_j^V$ and enthalpies $\tilde{H}_j^{VL}$ and $\tilde{H}_j^{VV}$, respectively.

To differentiate various streams, the following sets are defined:

Liquid streams

$\Gamma_1^L = \{i \ni L_i$ is saturated; route DN − MEN − DN$\}$

$\Gamma_2^L = \{i \ni L_i$ is subcooled; route DN – HEN(cold) – DN$\}$

$\Gamma_3^L = \{i \ni L_i$ is subcooled; route DN – HEN(hot) – DN$\}$

$\Gamma_4^L = \{i \ni L_i$ is saturated; route DN – MEN – HEN(hot) – DN$\}$

$\Gamma_5^L = \{i \ni L_i$ is saturated; route DN – MEN – HEN(cold) – PS – DN$\}$

$\Gamma_6^L = \{i \ni L_i$ is saturated; route DN – HEN(cold) – PS – DN$\}$

$I_1 = \{i \ni L_i$ goes to MEN I$\}$

$I_2 = \{i \ni L_i$ goes to MEN II$\}$

Vapor streams

$\Gamma_1^V = \{j \ni V_j$ is saturated stream; route DN – MEN – DN$\}$

$\Gamma_2^V = \{j \ni V_j$ is superheated; route DN – HEN(cold) – DN$\}$

$\Gamma_3^V = \{j \ni V_j$ is superheated; route DN – HEN(hot) – DN$\}$

$\Gamma_4^V = \{j \ni V_j$ is saturated; route DN – MEN – HEN(hot) – PS – DN$\}$

$\Gamma_5^V = \{j \ni V_j$ is saturated; route DN – MEN – HEN(cold) – DN$\}$

$\Gamma_6^V = \{j \ni V_j$ is saturated; route DN – HEN(hot) – PS – DN$\}$

$J_1 = \{j \ni V_j$ goes to MEN I$\}$

$J_2 = \{j \ni V_j$ goes to MEN II$\}$

Distribution network balances

Internal DN stream are denoted by a letter L or V which indicates the phases state of the stream. Supraindices LL, LV, VL, and VV indicate the origin and destination of the stream. Subindices give the number of the stream connected. For example, $L_{i,j}^{LV}$ stands for a liquid stream, which connects the inlet junction corresponding to liquid stream L_i and the outlet junction corresponding to vapor stream V_j. As two-phase stream can be formed at the outlet of the HEN, internal streams like $V_{i,j}^{LV}$ can exist, indicating that there is an internal vapor stream connecting the vapor outlet of a separator and a vapor stream. The inlet of this separator is a liquid stream in this case.

Material Balances at the Distribution Network: Splitting Junctions

$$L_i - \sum_{s=1}^{n_L} L_{i,s}^{LL} - \sum_{q=1}^{n_V} L_{i,q}^{LV} - \sum_{s=1}^{n_P} L_{i,r}^{LP} = 0 \quad i \in \Gamma_1^L, \Gamma_2^L, \Gamma_3^L, \Gamma_4^L$$

$$V_j - \sum_{i=1}^{n_L} V_{j,s}^{VL} - \sum_{q=1}^{n_V} V_{j,q}^{VV} - \sum_{r=1}^{n_P} V_{j,r}^{VP} = 0 \quad j \in \Gamma_1^V, \Gamma_2^V, \Gamma_3^V, \Gamma_5^V$$

$$V_i^L - \sum_{s=1}^{n_L} V_{i,s}^{LL} - \sum_{q=1}^{n_V} V_{i,q}^{LV} - \sum_{r=1}^{n_P} V_{i,r}^{LP} = 0 \quad i \in \Gamma_5^L, \Gamma_6^L$$

$$L_i^L - \sum_{s=1}^{n_t} L_{j,s}^{LL} - \sum_{q=1}^{n_V} L_{j,q}^{LV} - \sum_{r=1}^{n_P} L_{j,r}^{LP} = 0 \quad i \in \Gamma_5^L, \Gamma_6^L$$

$$V_j^V - \sum_{s=1}^{n_t} V_{j,s}^{VL} - \sum_{q=1}^{n_V} V_{j,q}^{VV} - \sum_{r=1}^{n_P} V_{j,r}^{VP} = 0 \quad j \in \Gamma_4^V, \Gamma_6^V$$

$$L_j^V - \sum_{i=1}^{n_L} L_{j,s}^{VL} - \sum_{q=1}^{n_V} L_{j,q}^{VV} - \sum_{r=1}^{n_P} L_{j,r}^{VP} = 0 \quad j \in \Gamma_4^V, \Gamma_6^V$$

$$\sum_{s=1}^{n_L} F_{n,s}^L + \sum_{q=1}^{n_V} F_{n,q}^V + \sum_{r=1}^{n_P} F_{n,r}^P - F_n = 0 \quad n = 1, \ldots, n_F$$

Mixing Junctions

Similarly, streams that are leaving the distribution network satisfy total mass component and energy balances. The corresponding equations are:

Material Balances

$$L_i - \sum_{s=1}^{n_L} L_{s,i}^{LL} - \sum_{s=n_{L4}+1}^{n_L} V_{s,i}^{LL} - \sum_{q=1}^{n_V} V_{q,i}^{VL} - \sum_{q=n_{V3}+1}^{n_{V4}} L_{q,i}^{VL} - \sum_{q=n_{V5}+1}^{n_V} L_{q,i}^{VL} - \sum_{n=1}^{n_F} F_{n,i}^L = 0 \quad \forall i$$

$$V_j - \sum_{s=1}^{n_L} L_{s,j}^{LV} - \sum_{s=n_{L4}+1}^{n_L} V_{q,j}^{LV} - \sum_{q=1}^{n_V} V_{q,j}^{VV} - \sum_{q=n_{V3}+1}^{n_{V4}} L_{q,i}^{VV} - \sum_{q=n_{V5}+1}^{n_V} L_{q,i}^{VV} - \sum_{n=1}^{n_F} F_{n,j}^V = 0 \quad \forall j$$

$$P_r - \sum_{s=1}^{n_L} L_{s,r}^{LP} - \sum_{s=n_{L4}+1}^{n_L} V_{s,r}^{VP} - \sum_{q=1}^{n_V} V_{q,r}^{VP} - \sum_{q=n_{V3}+1}^{n_{V4}} L_{q,r}^{VP} - \sum_{q=n_{V5}+1}^{n_V} L_{q,r}^{VP} - \sum_{n=1}^{n_F} F_{n,r}^P = 0 \quad \forall r$$

Key Component Balances

$$L_i x_i - \sum_{s=1}^{n_{L1}} L_{s,i}^{LL} \hat{x}_s - \sum_{s=n_{L1}+1}^{n_{L3}} L_{s,i}^{LL} x_s - \sum_{s=n_{L3}+1}^{n_{L4}} L_{s,i}^{LL} \hat{x}_s^L - \sum_{s=n_{L4}+1}^{n_L} L_{s,i}^{LL} \tilde{x}_s^L - \sum_{s=n_{L4}+1}^{n_L} V_{s,i}^{LL} \tilde{y}_s^L - \sum_{q=1}^{n_{V1}} V_{q,i}^{VL} \hat{y}_q - \sum_{q=n_{V1}+1}^{n_{V3}} V_{q,i}^{VL} y_q - \sum_{q=n_{V4}+1}^{n_{V5}} V_{q,i}^{VL} \hat{y}_q - \sum_{q=n_{V3}+1}^{n_{V4}} V_{q,i}^{VL} \tilde{y}_q^V \quad \forall i$$

$$- \sum_{q=n_{V3}+1}^{n_{V4}} L_{q,i}^{VL} \tilde{x}_q^V - \sum_{q=n_{V5}+1}^{n_V} V_{q,i}^{VL} \tilde{y}_q^V - \sum_{q=n_{V5}+1}^{n_V} L_{q,i}^{VL} \tilde{x}_q^V - \sum_{n=1}^{n_F} F_{n,i}^L z_n = 0$$

$$V_j y_j - \sum_{s=1}^{n_{L1}} L_{s,j}^{LV} \hat{x}_s - \sum_{s=n_{L1}+1}^{n_{L3}} L_{s,j}^{LV} x_s - \sum_{s=n_{L3}+1}^{n_{L4}} L_{s,j}^{LV} \hat{x}_s^L - \sum_{s=n_{L4}+1}^{n_L} L_{s,j}^{LV} \tilde{x}_s^L - \sum_{s=n_{L4}+1}^{n_L} V_{s,j}^{LV} \tilde{y}_s^L - \sum_{q=1}^{n_{V1}} V_{q,j}^{VV} \hat{y}_q - \sum_{q=n_{V1}+1}^{n_{V3}} V_{q,j}^{VV} y_q - \sum_{q=n_{V4}+1}^{n_{V5}} V_{q,j}^{VV} \hat{y}_q - \sum_{q=n_{V3}+1}^{n_{V4}} V_{q,j}^{VV} \tilde{y}_q^V \quad \forall j$$

$$- \sum_{q=n_{V3}+1}^{n_{V4}} L_{q,j}^{VV}\hat{x}_q^V - \sum_{q=n_{V5}+1}^{n_V} V_{q,j}^{VV}\hat{y}_q^V - \sum_{q=n_{V5}+1}^{n_V} L_{q,j}^{VV}\hat{x}_q^V - \sum_{n=1}^{n_F} F_{n,j}^V z_n = 0 \quad \forall j$$

$$P_r w_r - \sum_{s=1}^{n_{L1}} L_{s,r}^{LP}\hat{x}_s - \sum_{s=n_{L1}+1}^{n_{L3}} L_{s,r}^{LP}x_s - \sum_{s=n_{L3}+1}^{n_{L4}} L_{s,r}^{LP}\hat{x}_s^L - \sum_{s=n_{L4}+1}^{n_L} L_{s,r}^{LP}\tilde{x}_s^L - \sum_{s=n_{L4}+1}^{n_L} V_{s,r}^{LP}\tilde{y}_s^L - \sum_{q=1}^{n_{V1}} V_{q,r}^{VP}\hat{y}_q - \sum_{q=n_{V1}+1}^{n_{V3}} V_{q,r}^{VP}y_q - \sum_{q=n_{V5}+1}^{n_{V4}} V_{q,r}^{VP}\hat{y}_q - \sum_{q=n_{V3}+1}^{n_{V4}} V_{q,r}^{VP}\tilde{y}_q^V - \sum_{q=n_{V3}+1}^{n_{V4}} L_{q,r}^{VP}\tilde{x}_q^V - \sum_{q=n_{V5}+1}^{n_V} V_{q,r}^{VP}\tilde{y}_q^V - \sum_{q=n_{V5}+1}^{n_V} L_{q,r}^{VP}\tilde{x}_q^V - \sum_{n=1}^{n_F} F_{n,r}^P z_n = 0 \quad \forall r$$

Energy Balances

In the energy balances, provision has been made to include the change of enthalpy associated with a compression of a vapor stream. This change which is neglected in the case of liquids, is denoted by ω with respective supraindices and subindices indicating the starting and end junctions of the internal DN stream.

$$L_i H_i^L - \sum_{s=1}^{n_{L1}} L_{s,i}^{LL}\hat{H}_s^L - \sum_{s=n_{L1}+1}^{n_{L4}} L_{s,i}^{LL}\tilde{H}_s^L - \sum_{s=n_{L4}+1}^{n_L} L_{s,i}^{LL}\tilde{H}_s^{LL} - \sum_{s=n_{L4}+1}^{n_L} V_{s,i}^{LL}[\tilde{H}_s^{LV} + \omega_{s,i}^{LL}] - \sum_{q=1}^{n_{V1}} V_{q,i}^{VL}[\hat{H}_q^V + \omega_{q,i}^{VL}] - \sum_{q=n_{V1}+1}^{n_{V3}} V_{q,i}^{VL}[\tilde{H}_q^V + \omega_{q,i}^{VL}] - \sum_{q=n_{V3}+1}^{n_{V4}} V_{q,i}^{VL}[\tilde{H}_q^{VV} + \omega_{q,i}^{VL}] - \sum_{q=n_{V5}+1}^{n_V} L_{q,i}^{VL}\tilde{H}_q^{VL} - \sum_{q=n_{V4}+1}^{n_{V5}} V_{q,i}^{VL}[\tilde{H}_q^V + \omega_{q,i}^{VL}] \quad \forall i$$

$$- \sum_{q=n_{V5}+1}^{n_V} V_{q,i}^{VL}[\tilde{H}_q^{VV} + \omega_{q,i}^{VL}] - \sum_{q=n_{V3}+1}^{n_{V4}} L_{q,i}^{VL}\tilde{H}_q^{VL} - \sum_{n=1}^{n_F} F_{n,i}^L[H_n^F + \omega_{n,i}^{FL}] = 0$$

$$V_i H_j^V - \sum_{s=1}^{n_{L1}} L_{s,j}^{LV}\hat{H}_s^L - \sum_{s=n_{L1}+1}^{n_{L4}} L_{s,j}^{LV}\tilde{H}_s^L - \sum_{s=n_{L4}+1}^{n_L} L_{s,j}^{LV}\tilde{H}_s^{LL} - \sum_{s=n_{L4}+1}^{n_L} V_{s,j}^{LV}[\tilde{H}_s^{LV} + \omega_{s,j}^{LV}] - \sum_{q=1}^{n_{V1}} V_{q,j}^{VV}[\hat{H}_q^V + \omega_{q,j}^{VV}] - \sum_{q=n_{V1}+1}^{n_{V3}} V_{q,j}^{VV}[\tilde{H}_q^V + \omega_{q,j}^{VV}] - \sum_{q=n_{V3}+1}^{n_{V4}} V_{q,j}^{VV}[\tilde{H}_q^{VV} + \omega_{q,j}^{VV}]$$

$$- \sum_{q=n_{V3}+1}^{n_{V4}} L_{q,j}^{VV}\tilde{H}_q^{VL} - \sum_{q=n_{V4}+1}^{n_{V5}} V_{q,j}^{VV}[\tilde{H}_q^V + \omega_{q,j}^{VV}] - \sum_{q=n_{V5}+1}^{n_V} V_{q,j}^{VV}[\tilde{H}_q^{VV} + \omega_{q,j}^{VV}] - \sum_{q=n_{V5}+1}^{n_V} L_{q,j}^{VV}\tilde{H}_q^{VL} - \sum_{n=1}^{n_F} F_{n,j}^V[H_n^F + \omega_{n,j}^{FV}] = 0 \quad \forall j$$

$$\sum_{s=1}^{n_{L1}} L_{s,r}^{LP}\hat{H}_s^L + \sum_{s=n_{L1}+1}^{n_{L4}} L_{s,r}^{LP}\tilde{H}_s^L + \sum_{s=n_{L4}+1}^{n_L} L_{s,r}^{LP}\tilde{H}_s^{LL} + \sum_{s=n_{L4}+1}^{n_L} V_{s,r}^{LP}[\tilde{H}_s^{LV} + \omega_{s,r}^{LP}] + \sum_{q=1}^{n_{V1}} V_{q,r}^{VP}[\hat{H}_q^V + \omega_{q,r}^{VP}] + \sum_{q=n_{V1}+1}^{n_{V3}} V_{q,r}^{VP}[\tilde{H}_q^V + \omega_{q,r}^{VP}] + \sum_{q=n_{V3}+1}^{n_{V4}} V_{q,r}^{VP}[\tilde{H}_q^{VV} + \omega_{q,r}^{VP}] + \sum_{q=n_{V3}+1}^{n_{V4}} L_{q,i}^{VP}\tilde{H}_q^{VL} + \sum_{q=n_{V4}+1}^{n_{V5}} V_{q,r}^{VP}[\tilde{H}_q^V + \omega_{q,r}^{VP}] + \sum_{q=n_{V5}+1}^{n_V} V_{q,r}^{VP}[\tilde{H}_q^{VV} + \omega_{q,r}^{VP}] + \sum_{q=n_{V5}+1}^{n_V} L_{q,r}^{VP}\tilde{H}_q^{VL} + \sum_{n=1}^{n_F} F_{n,r}^P[H_n^F + \omega_{n,r}^{FP}] - P_r H_r^P = 0 \quad \forall r$$

Constraints for the phase state of streams

Phase changes are not allowed in the HEN, so that every stream is constrained to have a certain phase state. When a phase change takes place, it utilizes more than one stream.

In general, enthalpies are functions of composition, temperature and pressure. In particular, for ideal mixtures they are linear in concentration, with the coefficients depending on pressure. Thus:

Two Phase Streams at the Inlet of Separators (Outlet of HEN)

$$\begin{aligned}
\tilde{H}_i^L - b_i^{LV}\hat{x}_i &\le a_i^{LV} \quad i \in \Gamma_5^L, \Gamma_6^L \\
\tilde{H}_i^L - b_i^{LL}\hat{x}_i &\ge a_i^{LL} \quad i \in \Gamma_5^L, \Gamma_6^L \\
\tilde{H}_j^V - b_j^{VV}\hat{y}_j &\le a_j^{VV} \quad j \in \Gamma_4^V, \Gamma_6^V \\
\tilde{H}_j^V - b_j^{VL}\hat{y}_j &\ge a_j^{VL} \quad j \in \Gamma_4^V, \Gamma_6^V
\end{aligned}$$

Superheated Vapor Streams at the Inlet of the Distribution Network.

$$\tilde{H}_j^V - b_j^{VV}y_j \ge a_j^{VV} \quad j \in \Gamma_3^V$$

Subcooled Liquid Streams at the Inlet of the Distribution Network.

$$\tilde{H}_i^V - b_i^{LL}x_i \le a_i^{LL} \quad i \in \Gamma_2^L$$

Saturated Streams at the Outlet of the DN

$$H_i^L - b_i^{LL} x_i = a_i^{LL} \quad i \in \Gamma_1^L, \Gamma_4^L, \Gamma_5^L, \Gamma_6^L$$
$$H_j^V - b_j^{VV} y_j = a_j^{VV} \quad j \in \Gamma_1^V, \Gamma_4^V, \Gamma_5^V, \Gamma_6^V$$

Subcooled Liquids at the Outlet of the DN

$$H_i^L - b_i^{LL} x_i \le a_i^{LL} \quad i \in \Gamma_3^L$$

Superheated Vapors at the Outlet of the DN

$$H_j^V - b_j^{VV} y_j \ge a_j^{VV} \quad j \in \Gamma_2^V$$

Saturated Streams at the Outlet of the MEN

All streams at the outlet of the MEN are saturated.

$$\hat{H}_i^L - b_i^{LL} \hat{x}_i = a_i^{LL} \quad i \in \Gamma_1^L, \Gamma_4^L, \Gamma_5^L$$
$$\hat{H}_j^V - b_j^{VV} \hat{y}_j = a_j^{VV} \quad j \in \Gamma_1^V, \Gamma_4^V, \Gamma_5^V$$

Temperature-defining constraints

Temperature calculations are needed to write the feasibility constraints in the HEN. For simplicity, two-phase streams are assigned one single temperature. Dew points are chosen for cold streams and bubble points for hot streams.

HEN Inlet Streams

$$\left.\begin{aligned} T_i^L &= T_{\text{bub}_i}^L + \frac{(H_i^L - H_{\text{bub}_i}^L)}{cp_i^L} \\ T_{\text{bub}_i}^L &= c_{1i}^L + c_{2i}^L x_i + c_{3i}^L x_i^2 + c_{4i}^L x_i^3 \\ H_{\text{bub}_i}^L &= a_i^{LL} + b_i^{LL} x_i \end{aligned}\right\} \quad i \in \Gamma_2^L, \Gamma_3^L$$

$$\left.\begin{aligned} T_i^L &= T_{\text{bub}_i}^L + \frac{(\hat{H}_i^L - H_{\text{bub}_i}^L)}{cp_i^L} \\ T_{\text{bub}_i}^L &= c_{1i}^L + c_{2i}^L \hat{x}_i + c_{3i}^L \hat{x}_i^2 + c_{4i}^L \hat{x}_i^3 \\ H_{\text{bub}_i}^L &= a_i^{LL} + b_i^{LL} \hat{x}_i \end{aligned}\right\} \quad i \in \Gamma_4^L$$

$$\left.\begin{aligned} T_j^V &= T_{\text{dew}_j}^V + \frac{(H_j^V - H_{\text{dew}_j}^V)}{cp_j} \\ T_{\text{dew}_j}^V &= d_{1j}^V + d_{2j}^V y_j + d_{3j}^V y_j^2 + d_{4j}^V y_j^3 \\ H_{\text{dew}_j}^V &= a_j^{VV} + b_j^{VV} y_i \end{aligned}\right\} \quad j \in \Gamma_2^V, \Gamma_3^V$$

$$\left.\begin{aligned} T_j^V &= T_{\text{dew}_j}^V + \frac{(\hat{H}_j^V - H_{\text{dew}_j}^V)}{cp_j} \\ T_{\text{dew}_j}^V &= d_{1j}^V + d_{2j}^V \hat{y}_j + d_{3j}^V \hat{y}_j^2 + d_{4j}^V \hat{y}_j^3 \\ H_{\text{dew}_j}^V &= a_j^{VV} + b_j^{VV} \hat{y}_i \end{aligned}\right\} \quad j \in \Gamma_5^V$$

$$T_i^L = d_{1i}^L + d_{2i}^L \hat{x}_i + d_{3i}^L \hat{x}_i^2 + d_{4i}^L \hat{x}_i^3 \quad i \in \Gamma_5^L$$
$$T_i^L = d_{1i}^L + d_{2i}^L x_i + d_{3i}^L x_i^2 + d_{4i}^L x_i^3 \quad i \in \Gamma_6^L$$
$$T_j^V = c_{1j}^V + c_{2j}^V \hat{y}_j + c_{3j}^V \hat{y}_j^2 + c_{4j}^V \hat{y}_j^3 \quad j \in \Gamma_4^V$$
$$T_j^V = c_{1j}^V + c_{2j}^V y_j + c_{3j}^V y_j^2 + c_{4j}^V y_j^3 \quad j \in \Gamma_6^V$$

HEN Outlet Streams

$$\tilde{T}_i^L = T_{\text{bub}_i}^L + \frac{(\tilde{H}_i^L - H_{\text{bub}_i}^L)}{cp_i^L} \quad i \in \Gamma_2^L, \Gamma_3^L, \Gamma_4^L$$

$$\tilde{T}_j^V = T_{\text{dew}_j}^V + \frac{(\tilde{H}_j - H_{\text{dew}_j}^V)}{cp_j} \quad j \in \Gamma_2^V, \Gamma_3^V, \Gamma_5^V$$

Rich- and lean-stream definition

Rich Streams

$$\hat{x}_i - x_i \le 0 \quad i \in \Gamma_1^L, \Gamma_4^L, \Gamma_5^L$$

Lean Streams

$$\hat{y}_j - y_j \le 0 \quad j \in \Gamma_1^V, \Gamma_4^V, \Gamma_5^V$$

Hot- and cold-stream definition

Hot Streams

$$\tilde{H}_i^L - H_i^L \le 0 \quad i \in \Gamma_3^L$$
$$\tilde{H}_i^L - \hat{H}_i^L \le 0 \quad i \in \Gamma_4^L$$
$$\tilde{H}_j^V - H_j^V \le 0 \quad j \in \Gamma_3^V$$
$$\tilde{H}_j^V - \hat{H}_j^V \le 0 \quad j \in \Gamma_4^V$$
$$\tilde{H}_j^V - H_j^V \le 0 \quad j \in \Gamma_6^V$$

Cold Streams

$$\tilde{H}_i^L - H_i^L \ge 0 \quad i \in \Gamma_2^L$$
$$\tilde{H}_i^L - \hat{H}_i^L \ge 0 \quad i \in \Gamma_5^L$$
$$\tilde{H}_i^L - H_i^L \ge 0 \quad i \in \Gamma_6^L$$
$$\tilde{H}_j^V - H_j^V \ge 0 \quad j \in \Gamma_2^V$$
$$\tilde{H}_j^V - \hat{H}_j^V \ge 0 \quad j \in \Gamma_5^V$$

Equations for the separators

Equilibrium Equations

$$\tilde{y}_i^L - F(\tilde{x}_i^L) = 0 \quad i \in \Gamma_5^L, \Gamma_6^L$$
$$\tilde{y}_j^V - F(\tilde{x}_j^V) = 0 \quad j \in \Gamma_4^V, \Gamma_6^V$$

The constant volatility expression is used for $F(x)$.

Enthalpy Equations (Outlet Streams)

$$\tilde{H}_i^{LV} - b_i^{LV} \tilde{y}_i^L = a_i^{LV} \quad i \in \Gamma_5^L, \Gamma_6^L$$
$$\tilde{H}_i^{LL} - b_i^{LL} \tilde{x}_i^L = a_i^{LL} \quad i \in \Gamma_5^L, \Gamma_6^L$$
$$\tilde{H}_j^{VV} - b_j^{VV} \tilde{y}_j^V = a_j^{VV} \quad i \in \Gamma_4^V, \Gamma_6^V$$
$$\tilde{H}_j^{VL} - b_j^{VL} \tilde{x}_j^V = a_j^{VL} \quad i \in \Gamma_4^V, \Gamma_6^V$$

Material, Component and Energy Balances

$$L_i - L_i^L - V_i^L = 0 \quad i \in \Gamma_5^L, \Gamma_6^L$$
$$V_j - L_j^V - V_j^V = 0 \quad j \in \Gamma_4^V, \Gamma_6^V$$
$$L_i \hat{x}_i - L_i^L \tilde{x}_i^L - V_i^L \tilde{y}_i^L = 0 \quad i \in \Gamma_5^L$$

$$
\begin{aligned}
L_i x_i - L_i^L \tilde{x}_i^L - V_i^L \tilde{y}_i^L = 0 \quad & i \in \Gamma_6^L \\
V_j \hat{y}_j - L_j^V \tilde{x}_j^V - V_j^V \tilde{y}_j^V = 0 \quad & j \in \Gamma_4^V \\
V_j y_j - L_j^V \tilde{x}_j^V - V_j^V \tilde{y}_j^V = 0 \quad & j \in \Gamma_6^V \\
L_i \tilde{H}_i^L - L_i^L \tilde{H}_i^{LL} - V_i^L \tilde{H}_i^{LV} = 0 \quad & i \in \Gamma_5^L, \Gamma_6^L \\
V_j \tilde{H}_j^V - L_j^V \tilde{H}_j^{VL} - V_j^V \tilde{H}_j^{VV} = 0 \quad & j \in \Gamma_4^V, \Gamma_6^V
\end{aligned}
$$

Pinch operator constraints (MEN)

Pinch inequality constraints are formalized in the following way:

Constraints for the Pinch candidate x_i (rich streams)
Let

$$
\begin{aligned}
s_{k,i} &= \text{Max}\{x_k,\ x_i\} \\
\hat{s}_{k,i} &= \text{Max}\{\hat{x}_k,\ x_i\} \\
r_{j,i} &= \text{Max}\{y_j,\ F(x_i) - \epsilon\} \\
\hat{r}_{j,i} &= \text{Max}\{\hat{y}_j,\ F(x_i) - \epsilon\}
\end{aligned}
$$

Then the pinch inequality is:

$$
L_i(x_i - \hat{x}_i) + \sum_{k \neq i, k \in I_1} L_k[(x_k - s_{k,i}) - (\hat{x}_k - \hat{s}_{k,i})] - \sum_{j \in J_1} V_j[(\hat{y}_j - \hat{r}_{j,i}) - (y_j - r_{j,i})] \leq 0 \quad i \in I_1
$$

$$
L_i(x_i - \hat{x}_i) + \sum_{k \neq i, k \in I_2} L_k[(x_k - s_{k,i}) - (\hat{x}_k - \hat{s}_{k,i})] - \sum_{j \in J_2} V_j[(\hat{y}_j - \hat{r}_{j,i}) - (y_j - r_{j,i})] \leq 0 \quad i \in I_2
$$

Since the following overall balance holds (there are no mass separating utilities)

$$
\sum_i L_i(x_i - \hat{x}_i) - \sum_j V_j(\hat{y}_j - y_j) = 0
$$

then the pinch inequalities become

$$
\sum_{k \neq i, k \in I_1} L_k(\hat{s}_{k,i} - s_{k,i}) - \sum_{j \in J_1} V_j(r_{j,i} - \hat{r}_{j,i}) \leq 0 \quad i \in I_1
$$

$$
\sum_{k \neq i, k \in I_2} L_j(\hat{s}_{k,i} - s_{k,i}) - \sum_{j \in J_2} V_j(r_{j,i} - \hat{r}_{j,i}) \leq 0 \quad i \in I_2
$$

Constraints for the Pinch candidate y_j (lean streams)
The inequalities are:

$$
\sum_{i \in I_1} L_i(\hat{p}_{i,j} - p_{i,j}) + V_j(\hat{y}_j - y_j) - \sum_{k \neq j, k \in J_1} V_k(t_{k,j} - \hat{t}_{k,j}) \leq 0 \quad j \in J_1
$$

$$
\sum_{i \in I_2} L_i(\hat{p}_{i,j} - p_{i,j}) + V_j(\hat{y}_j - y_j) - \sum_{k \neq j, k \in J_2} V_k(t_{k,j} - \hat{t}_{k,j}) \leq 0 \quad j \in J_2
$$

where

$$
\begin{aligned}
p_{i,j} &= \text{Max}\{x_i,\ G(y_j + \epsilon)\} \\
\hat{p}_{i,j} &= \text{Max}\{\hat{x}_i,\ G(y_j + \epsilon)\} \\
t_{k,j} &= \text{Max}\{y_k,\ y_j\} \\
\hat{t}_{k,j} &= \text{Max}\{\hat{y}_k,\ y_j\}
\end{aligned}
$$

The following set of linear constraints is used to calculate the maximum of two numbers.

$$
C = \text{Max}(A,B) \Leftrightarrow \begin{cases} A + \lambda\Gamma \geq C \\ C \geq A \\ B + (1-\lambda)\Gamma \geq C \\ C \geq B \end{cases}
$$

Pinch operator constraints (HEN)

Let G_k represent all hot streams and C_s all cold streams. Let also T_k^G, $\tilde{T}_k^G$, and T_s^C, $\tilde{T}_s^C$, represent the HEN inlet and outlet temperatures of the hot and cold streams, respectively. Similarly, let H_k^G, $\tilde{H}_k^G$, and H_s^C, $\tilde{H}_s^C$ represent the HEN inlet and outlet temperatures of the hot and cold streams, respectively. Enthalpy functions for hot and cold streams are given by $Z_k^G(T)$ and $Z_s^C(T)$, respectively. Let us also define the following sets:

$$
\begin{aligned}
K &= \{i \ni L_i \text{ or } V_i \text{ is a hot stream}\} \\
S &= \{i \ni L_i \text{ or } V_i \text{ is a cold stream}\}
\end{aligned}
$$

Constraints for the Pinch candidate T_k^G (hot streams)
Let

$$
\begin{aligned}
R_{m,k} &= \text{Max}\{T_m^G,\ T_k^G\} \\
\tilde{R}_{m,k} &= \text{Max}\{\tilde{T}_m^G,\ T_k^G\} \\
U_{s,k} &= \text{Max}\{T_s^C,\ T_k^G - \Delta T\} \\
\tilde{U}_{s,k} &= \text{Max}\{\tilde{T}_s^C,\ T_k^G - \Delta T\}
\end{aligned}
$$

Then, the pinch inequality is:

$$
\sum_{m \neq k, m \in K} G_m[(Z_m^G(\tilde{R}_{m,k}) - Z_m^G(R_{m,k})] - \sum_{s \in S} C_s[Z_s^C(U_{s,k}) - Z_s^C(\tilde{U}_{s,k})] \leq 0 \quad \forall k \in K
$$

Constraints for the Pinch candidate T_s^C (cold streams)
Let

$$
\begin{aligned}
M_{k,s} &= \text{Max}\{T_k^G,\ T_s^C + \Delta T\} \\
\tilde{M}_{k,s} &= \text{Max}\{\tilde{T}_k^G,\ T_s^C + \Delta T\} \\
N_{m,s} &= \text{Max}\{T_m^C,\ T_s^C\} \\
\tilde{N}_{m,s} &= \text{Max}\{\tilde{T}_m^C,\ T_s^C\}
\end{aligned}
$$

Then, the pinch inequality is:

$$
\sum_{k \in K} G_k[Z_k^G(\tilde{M}_{k,s}) - Z_k^G(M_{k,s})] + C_s(\tilde{H}_s^C - H_s^C) - \sum_{m \neq s, m \in S} C_m[Z_m^C(N_{m,s} - Z_m^C(\tilde{N}_{m,s})] \leq 0 \quad \forall s \in S
$$

Split-matching operator constraints

MEN Constraints
Let $Q_{i,j}^m$ be the mass exchanged between a rich (liquid) stream and a lean (vapor) stream. Then,

$$\sum_{i\in I_1} Q^m_{i,j} = V_j(\hat{y}_j - y_j) \qquad j\in J_1$$

$$\sum_{j\in J_1} Q^m_{i,j} = L_i(x_i - \hat{x}_i) \qquad i\in I_1$$

$$\sum_{i\in I_2} Q^m_{i,j} = V_j(\hat{y}_j - y_j) \qquad j\in J_2$$

$$\sum_{j\in J_2} Q^m_{i,j} = L_i(x_i - \hat{x}_i) \qquad i\in I_2$$

Feasibility constraints are:

$$\left.\begin{aligned} Q^m_{i,j}[(\hat{y}_j - F(x_i) + \epsilon] \le 0 \\ Q^m_{i,j}[y_j - F(\hat{x}_i) + \epsilon] \le 0 \end{aligned}\right\} \quad i\in I_1,\ j\in J_1$$

$$\left.\begin{aligned} Q^m_{i,j}[\hat{y}_j - F(x_i) + \epsilon] \le 0 \\ Q^m_{i,j}[y_j - F(\hat{x}_i) + \epsilon] \le 0 \end{aligned}\right\} \quad i\in I_2,\ j\in J_2$$

HEN Constraints

Let $Q^h_{k,s}$ be the heat exchanged between a hot stream and a cold stream. Then,

$$\sum_k Q^h_{k,s} = C_s(H^C_s - \tilde{H}^C_s) \qquad \forall k$$

$$\sum_s Q^h_{k,s} = G_k(H^G_k - \tilde{H}^G_k) \qquad \forall s$$

Feasibility constraints are:

$$Q^h_{k,s}[T^G_k - \tilde{T}^C_s + \Delta T] \ge 0$$
$$Q^h_{k,s}[\tilde{T}^G_k - \tilde{T}^C_s + \Delta T] \ge 0$$

Objective Function

Utility cost is a linear combination of hot utility (steam in most cases), cold utility (cooling water or refrigerants), flow rates and power consumption (compression of vapors). In this article we consider the use of Steam S, cooling water W, refrigerant R, and electrical power E.

Let c_S, c_E, c_R, and c_E be the cost of steam, cooling water, refrigerant fluid and electricity respectively. The total utility cost to minimize is then given by:

$$C = c_S S + c_W W + c_R R + c_E E$$

Manuscript received Sept. 24, 1991, and revision received June 5, 1992.